REPORT

BRAIN RESEARCH

Causal neural network of metamemory for retrospection in primates

Kentaro Miyamoto,[1] Takahiro Osada,[1,2] Rieko Setsuie,[1]* Masaki Takeda,[1,2]* Keita Tamura,[1] Yusuke Adachi,[1] Yasushi Miyashita[1,2]†

We know how confidently we know: Metacognitive self-monitoring of memory states, so-called "metamemory," enables strategic and efficient information collection based on past experiences. However, it is unknown how metamemory is implemented in the brain. We explored causal neural mechanism of metamemory in macaque monkeys performing metacognitive confidence judgments on memory. By whole-brain searches via functional magnetic resonance imaging, we discovered a neural correlate of metamemory for temporally remote events in prefrontal area 9 (or 9/46d), along with that for recent events within area 6. Reversible inactivation of each of these identified loci induced doubly dissociated selective impairments in metacognitive judgment performance on remote or recent memory, without impairing recognition performance itself. The findings reveal that parallel metamemory streams supervise recognition networks for remote and recent memory, without contributing to recognition itself.

Introspection on memory states (*1*), or self-monitoring (*2*, *3*) and evaluation (*3*–*5*) of our own memory (*6*), makes us feel retrospective. This self-reflective mental process had been commonly believed to be unique to humans because it requires a higher level of cognition about our own cognition. This meta-level memory process is termed "metamemory" (*1*, *6*–*8*), and is conceptually considered to supervise the process of memory execution itself (i.e., encoding, maintenance, and retrieval). However, the neural mechanism of metamemory, even the cortical distribution of responsible neural activities, is totally unknown, whereas the neural basis of memory execution has been precisely revealed as a multitiered brain-wide network in humans and animals (*1*, *6*, *9*, *10*). Therefore, it remains elusive whether and, if so, how metamemory is implemented in the brain as an independent and integrative neural process that is distinct from the memory execution process itself.

For exploration of unknown neural substrates, it is efficient and fruitful to combine whole-brain searches for neural correlates and subsequent examinations of causal behavioral impacts by finely targeted neural intervention (*11*). The psychological and behavioral framework for experimentation on metacognitive skills has been developed only recently in nonlinguistic animals (*12*, *13*). Studies in rats (*14*) and macaques (*15*–*17*) recorded neuronal activity that was related to the metacognitive judgment on perception rather than on memory. These studies identified the neural correlates of the self-monitoring skills used to make adaptive decisions based on real-time experiences: Single-cell activity carried information that correlated with both perceptual metacognition and perception itself (*14*–*17*). In contrast, metamemory requires the reconstruction of past experiences as present mental representations and, thus, naturally requires more self-reflective and introspective information processing than perceptual metacognition. We developed a nonhuman primate neurobiological model of metamemory using macaque monkeys, because—together with apes and dolphins—they are the only animals besides humans that were recently demonstrated to exhibit metamnemonic skills (*12*, *13*). Both whole-brain searches and finely targeted neuronal interventions can be applied to macaque monkeys (Fig. 1A).

Monkeys were required to perform a yes/no visual memory recognition test (*13*, *18*, *19*) (memory stage; Fig. 1B) and to make self-confidence judgments regarding their own retrieved memory (*20*) using the postdecision wagering paradigm (*17*) (bet stage; Fig. 1B). In the memory stage, recognition performance for the cue item at each position (OLD1 to OLD4) was significant [corrected recognition rate (hit rate − false alarm rate): $t_{31} > 3.42$, $P < 0.008$, corrected for multiple comparisons with Bonferroni's test] [Fig. 2A (left)]. Correct response rates exhibited U-shaped serial position curves (*18*) with both a significant primacy effect [first item (OLD1) versus middle items (OLD2 and OLD3): $t_{31} = 2.38$, $P = 0.023$, Bonferroni's correction, following analysis of variance (ANOVA), $F_{3,90} = 2.93$, $P = 0.037$] and a significant recency effect [last item (OLD4) versus middle items (OLD2 and OLD3): $t_{31} = 2.39$, $P = 0.022$]. These results were confirmed by d' of type I signal detection theory ($t_{31} = 4.71$, $P = 4.9 \times 10^{-10}$) [Fig. 2A (right) and fig. S1A]. Responses for successful retrieval of the last item were faster than those of the other items [OLD4 versus OLD1, OLD2, OLD3: $t_{31} > 2.17$ $P < 0.05$ corrected for multiple comparison with Holm's test; recent OLD (OLD4) versus remote OLD (OLD1, OLD2, and OLD3): $t_{31} = 2.99$, $P = 0.0053$] (fig. S1B) and suggested that recent memory processes for retrieval of the latest items were distinct from remote memory processes for the initial three items. In the bet stage, the monkeys more frequently chose "high bets" when they correctly answered the precedent test than when they failed it ($t_{31} > 4.63$, $P < 1.8 \times 10^{-4}$ for both OLD and NEW conditions) (Fig. 2B). Confidence judgment performances evaluated by the phi coefficient (Φ) (*21*), a contingency table–based statistical index of preference for optimal choice, were significantly positive (Φ^{OLD}: $t_{31} = 5.60$, $P = 3.8 \times 10^{-6}$; Φ^{NEW}: $t_{31} = 5.60$, $P = 3.8 \times 10^{-6}$) (see also fig. S1C). Optimal choices in confidence judgment were also confirmed by significantly positive meta-d' (*22*) ($t_{31} = 9.37$, $P = 4.6 \times 10^{-10}$), an index based on type II signal detection theory, which was highly correlated with Φ across experimental days (sessions) [correlation coefficient (r) = 0.84, $P = 1.0 \times 10^{-9}$] (fig. S1D) (see methods for details). For the relation with the serial position effect, in the OLD1, OLD4, and NEW conditions, recognition performance was better for high-bet trials than for low-bet trials [main effect of confidence: $F_{1,30} = 35.4$, $P = 1.6 \times 10^{-6}$; high bet versus low bet: $t_{31} = 4.21$, $P = 6.0 \times 10^{-4}$ (OLD1); $t_{31} = 2.60$, $P = 0.042$ (OLD4); $t_{31} = 5.97$, $P = 3.9 \times 10^{-6}$ (NEW), Bonferroni's correction] (Fig. 2C). Moreover, high-bet preference was correlated with recognition performance across sessions ($r = 0.46$, $P = 0.0077$) (fig. S1E). Despite the longer response time for incorrect responses (incorrect versus correct: $t_{31} = 2.74$, $P = 0.010$), monkeys did not use response latency of the memory stage as an external behavioral cue for making a bet decision (high bet versus low bet: $t_{31} = 0.81$, $P = 0.42$ for correct trials; $t_{31} = 1.01$, $P = 0.32$ for incorrect trials) (Fig. 2D). Both the confidence judgment and recognition performance were consistent across monkeys (fig. S2).

Using whole-brain functional mapping, we identified cortical areas involved in metamemory processing by comparing brain activity between high-bet and low-bet trials in memory retrieval [Fig. 3, A and B, (left)] (see discussion for exclusion of possible components of reward or memory strength). The majority of the metamemory processing areas activated in OLD (hit) condition were localized within the dorsal prefrontal cortex, around the posterior supraprincipal dimple [$P < 0.05$, family-wise error correction (FWE) across the whole-brain volume] [Fig. 3A (right) and table S1A, see also fig. S3A], whereas those in NEW (correct rejection) condition were distributed within the posterior parietal cortex ($P < 0.05$, whole-brain corrected) [Fig. 3B (right) and table S1B; see also

[1]Department of Physiology, The University of Tokyo School of Medicine, 7-3-1 Hongo, Bunkyo-ku, Tokyo 113-0033, Japan. [2]Juntendo University Graduate School of Medicine, 2-1-1 Hongo, Bunkyo-ku, Tokyo 113-8421, Japan.
*These authors contributed equally to this work. †Corresponding author. Email: yasushi_miyashita@m.u-tokyo.ac.jp

Downloaded from http://science.sciencemag.org/ on October 27, 2017

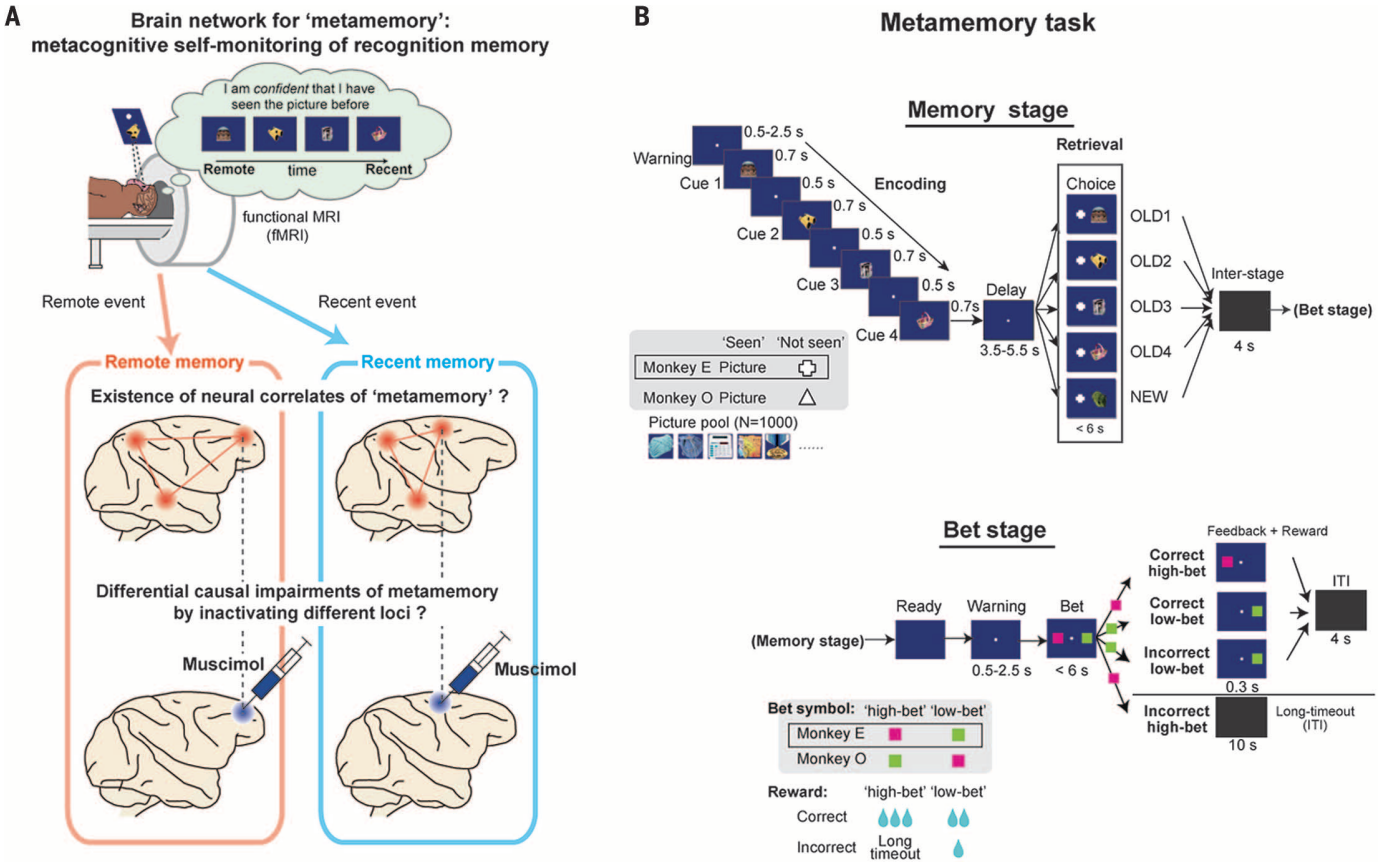

Fig. 1. Experimental design and metamemory task. (**A**) Whole-brain functional localization of metamemory networks for "remote" and "recent" events via functional magnetic resonance imaging (fMRI) and behavioral reversible inactivation with a $GABA_A$ receptor agonist (muscimol) in macaque monkeys performing a metamemory task. (**B**) Metamemory task sequence. In the memory stage, if the picture in the choice period was included in the encoded item list, monkeys were required to choose the picture (OLD condition); if not, they were to choose the "not seen" symbol (NEW condition). In the bet stage, monkeys were required to place either high or low bets on the basis of confidence about memory in a postdecision wagering paradigm.

fig. S3, A and B]. Overlap between the distributions of the OLD and NEW metamemory processing areas was marginal (fig. S3C). Because the behavioral results indicated that distinct memory processes operate for retrieval of the latest items (fig. S1B), metamemory processing areas were then examined for successful retrieval of remote memory (remote OLD) and recent memory (recent OLD) separately. For remote OLD condition, metamemory processing areas were localized bilaterally around the lateral area 9 and area 8B ($P < 0.05$, whole-brain corrected) (Fig. 3C and table S2A), especially on the region anteriorly from the posterior supraprincipal dimple (aPSPD) within area 9 and 9/46d. For recent OLD condition, metamemory-related activations were localized at anterior part of the supplementary eye field (SEFa) within area 6 (Fig. 3C and table S2B) ($P < 0.05$, whole-brain corrected). aPSPD was consistently activated for each of three remote items (OLD1, 2, and 3) ($P < 0.001$, Bonferroni's correction) [Fig. 3D (top)], but not for the last recent item, whereas SEFa was especially activated during retrieval of the last recent item ($P < 0.001$, Bonferroni's correction) [Fig. 3D (bottom)], but not for either of three remote items. Metacognitive roles for area 9, especially at aPSPD, have never been discovered before, although the contribution of supplementary eye field to perceptual metacognition has been suggested (*17*) (for roles of SEF, see supplementary text). We then examined how activity within each metamemory processing area contributed to behavioral performance in confidence judgment by calculating the session-by-session correlation between task-evoked functional magnetic resonance imaging (fMRI) activity and Φ index (Fig. 3E). We identified aPSPD as the locus for the remote items ($r = 0.48$, $P = 0.0047$, Bonferroni's correction), but not for the recent or new items. In contrast, the SEFa was identified as the locus for the recent item ($r = 0.38$, $P = 0.045$, Bonferroni's correction), but not for the remote or new items (for direct comparisons of these correlations see fig. S6A). fMRI activity in the other metamemory processing areas localized for remote OLD and recent OLD conditions could not predict performance for any items (Fig. 3F). Metamemory-related activities in aPSPD and SEFa (fig. S4), and their contribution to confidence judgment performance (fig. S6B), were consistent across monkeys (see also table S4 and fig. S5 for the whole-brain activities in each monkey).

Next, we examined how these metamnemonic loci interact with other areas during the metamemory task by psychophysiological interaction (PPI). Activity in aPSPD was dominantly coupled with area PG in the inferior parietal lobule for metamnemonic judgment on remote items (Fig. 3G and table S3) ($P < 0.05$, false discovery rate corrected at cluster level across the whole brain), whereas activity in SEFa was dominantly coupled with area PEa in the superior parietal lobule for metamnemonic judgment on recent items (Fig. 3G and table S3) ($P < 0.05$, cluster-level corrected). Area PG and area PEa were also active during retrieval of remote or recent items, respectively, in an identical recognition memory test without wagering (*18*).

Finally, to examine the direct causal impact of neuronal activity in aPSPD or SEFa on metamnemonic performance, we bilaterally microinjected a γ-aminobutyric acid receptor type A ($GABA_A$ receptor) agonist (muscimol) separately into each of these loci (Fig. 4A) and evaluated the severity of impairment in confidence judgment by comparing Φ after injection and Φ before injection [ΔΦ = Φ(POST injection) – Φ(PRE injection)] for remote OLD ($\Delta\Phi^{Remote}$), recent OLD ($\Delta\Phi^{Recent}$), and NEW ($\Delta\Phi^{New}$) conditions, separately. The results demonstrated doubly dissociated behavioral impairments in confidence judgment between the loci: Comparisons of ΔΦ

Downloaded from http://science.sciencemag.org/ on October 27, 2017

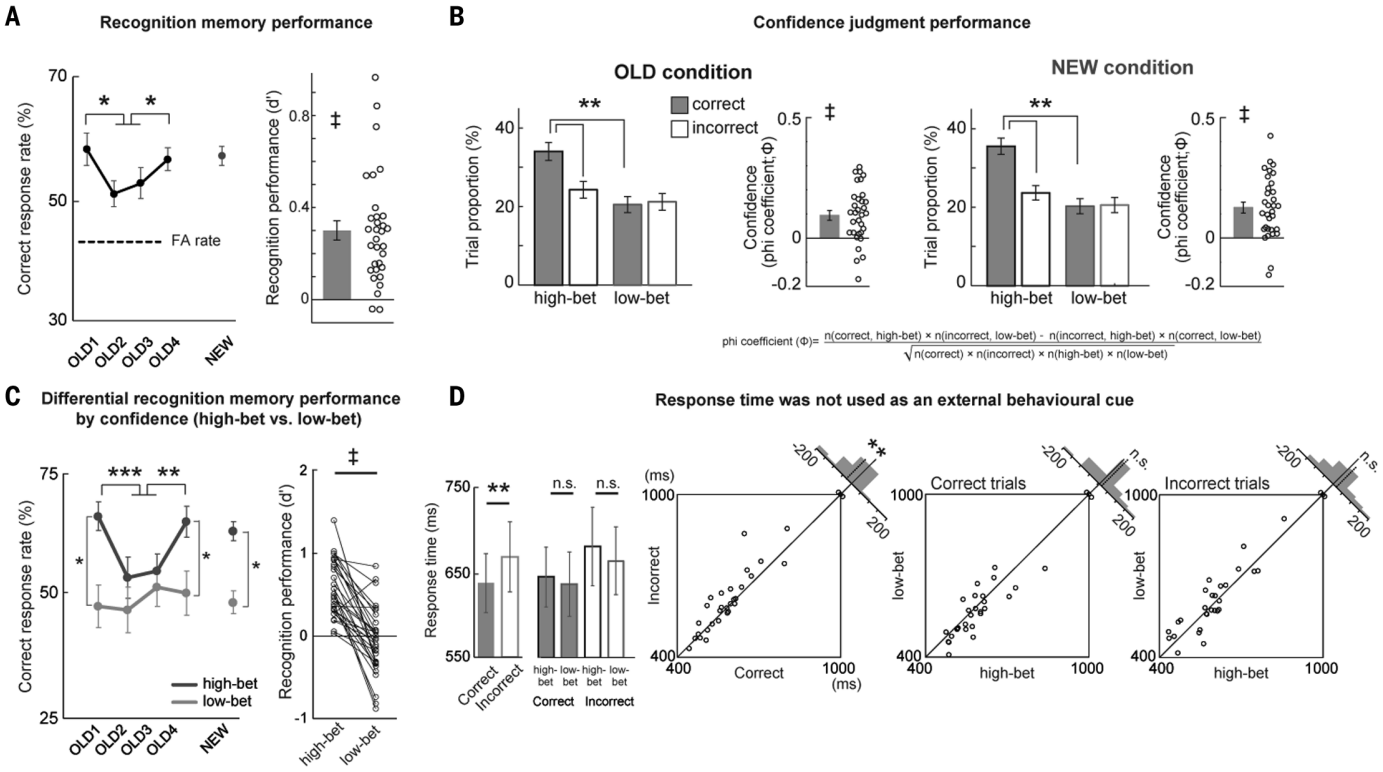

Fig. 2. Behavioral performance of metamemory task. (**A**) Recognition memory performance. (Left) Serial position curve of correct response rate with significant primacy and recency effects. *P < 0.05, paired t test (Bonferroni's correction). (Right) The d' of signal detection theory. ‡P < 0.001, t test against zero. (**B**) Confidence judgment performance evaluated by trial proportion and phi coefficient (Φ). **P < 0.01, paired t test (Bonferroni's correction). ‡P < 0.001, t test against zero. (**C**) Recognition performance in high- and low-bet trials. (Left) Correct response rates for high-bet (dark gray) and low-bet (light gray) trials. *P < 0.05, **P < 0.01, ***P < 0.001, paired t test (Bonferroni's correction). (Right) Differences in d' of signal-detection theory between high- and low-bet trials. ‡P < 0.001, paired t test. (**D**) Differences in response time according to recognition performance (correct or incorrect) and confidence judgment (high bet or low bet). (Left bar graphs) Response time. **P = 0.01, paired t test. No significant interaction (correct or incorrect × high bet or low bet) was found in either of the animals (monkey E: $F_{1,15}$ = 0.17, P = 0.67; monkey O: $F_{1,15}$ = 1.51, P = 0.23). (Right scatter plots) Relation of session-by-session response times for labeled conditions. Each open circle in this figure represents a single session (N = 32). Histograms show distribution of session-by-session difference. Dotted line denotes mean. Error bars denote SEM.

showed a significant interaction between injected loci and memory task conditions [(aPSPD and SEFa) × (remote OLD, recent OLD, NEW); $F_{2,28}$ = 5.95, P = 0.007] (Fig. 4B), with no difference in impairment between monkeys (interaction for injected loci × memory conditions × monkeys; $F_{2,28}$ = 0.32, P = 0.72). This double-dissociation was confirmed by the signal-detection theory-based metacognitive efficiency index [Δ(meta-d' – d')] (*22*) (interaction for injected loci × memory task conditions: $F_{1,7}$ = 6.41; P = 0.039) (fig. S7B). aPSPD injections evoked a significantly greater metamnemonic impairment for remote OLD condition than for the other conditions ($\Delta\Phi^{Remote}$ versus $\Delta\Phi^{Recent}$ and $\Delta\Phi^{Remote}$ versus $\Delta\Phi^{New}$: P < 0.05, corrected with post hoc Ryan's test; $\Delta\Phi^{Recent}$ versus $\Delta\Phi^{New}$: P > 0.05), whereas SEFa injections evoked a significantly greater impairment for recent OLD condition than for the others ($\Delta\Phi^{Recent}$ versus $\Delta\Phi^{Remote}$ and $\Delta\Phi^{Recent}$ versus $\Delta\Phi^{New}$: P < 0.05, Ryan's correction; $\Delta\Phi^{Remote}$ versus $\Delta\Phi^{New}$: P > 0.05). Significant metamnemonic impairment was observed only in remote OLD condition of aPSPD injection ($\Delta\Phi^{Remote}$ < 0; t_8 = –6.29, P = 0.0014, Bonferroni's correction) (Fig. 4B) and in recent OLD condition of SEFa injection ($\Delta\Phi^{Recent}$ < 0; t_8 = –3.52, P = 0.046, Bonferroni's correction) [see also fig. S7A and C for session-by-session data and impairment evaluation by Φ(POST injection)]. In contrast, saline injection at aPSPD and SEFa did not result in any impairments in confidence judgments (t_7 < 0.48, P > 0.9; interaction for injected loci × memory task conditions: $F_{2,22}$ = 0.42, P = 0.66) (Fig. 4C). Notably, muscimol injection did not impair the recognition memory process itself: The difference between d' after injection and d' before injection ($\Delta d'$) was not significant under any condition (t_8 < 0.77, P > 0.9) (Fig. 4D) and showed no significant interaction between injected loci and recognition memory task conditions ($F_{1,14}$ = 0.002, P = 0.96). Additionally, a serial position curve with significant primacy and recency effects was retained even after muscimol injection (OLD1 versus OLD3, OLD4 versus OLD3: P < 0.05) [Fig. 4E (top)], and recognition memory performance remained statistically significant in all conditions (P < 0.05) [Fig. 4E (bottom)]. Both the results from whole-brain functional MRI mapping and causal behavioral tests reveal that the whole-brain metamemory process is composed not of a unitary stream but of parallel streams with multiple readout cores directing one-on-one remote and recent memory networks (Fig. 4F).

The following three lines of behavioral evidence demonstrate that monkeys performed this postdecision wagering metacognitive judgment task (Fig. 1B) on the basis of their confidence about memory. First, monkeys more frequently placed high bets after a successful performance on the preceding memory tasks (Fig. 2B and fig. S1, C and E), as confirmed by both the contingency table–based Φ (*17*) and signal detection theory–based meta-d' indices (*22*) (fig. S1D). Second, a serial position curve with significant primacy and recency effects was observed for high-bet, but not for low-bet, conditions (Fig. 2C); this corresponds with predictions from signal detection theory (*13*). Third, monkeys did not use response latency as a behavioral cue for making bet decisions (*20*) (Fig. 2D); this observation satisfies the established criterion required for demonstrations of animal metacognition in laboratory environment when using the postdecision wagering paradigm (*12*).

Metamemory signals derived from comparisons between high-bet and low-bet conditions in whole-brain imaging are at risk of confounding with reward-related signals (reward proper,

Downloaded from http://science.sciencemag.org/ on October 27, 2017

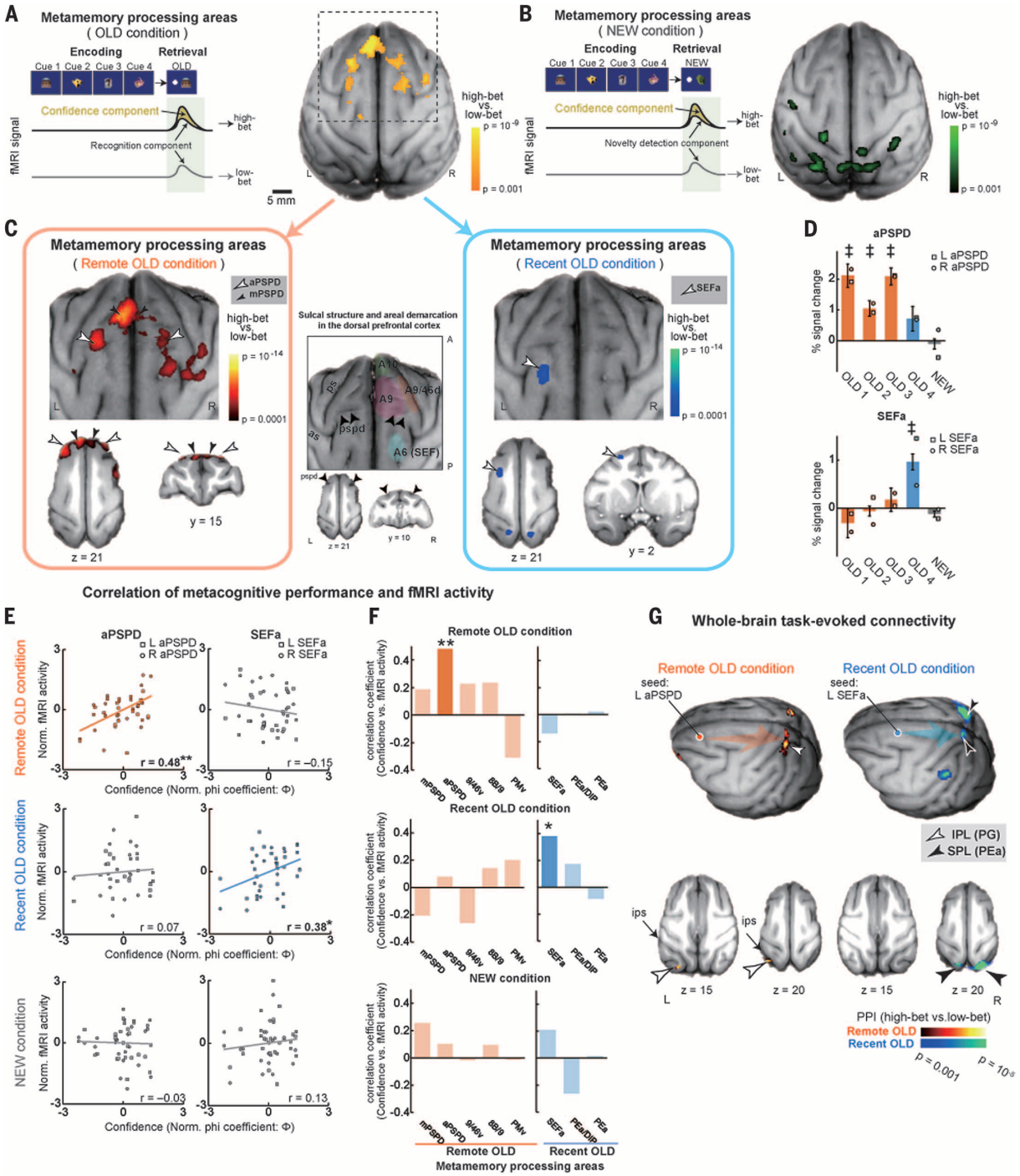

Fig. 3. Whole-brain functional mapping of metamemory network. (**A**) (Left) fMRI subtraction schema for metamemory-related signals (confidence components). (Right) metamemory processing areas for OLD conditions identified by the subtraction (high bet versus low bet; $z > 3.1$, $P < 0.001$, uncorrected for display purpose). Dashed line frames magnified brain region in (C). (**B**) Metamemory processing areas for NEW conditions. (**C**) (Left) Metamemory processing areas for remote OLD condition (OLD1–3) ($z > 3.7$, $P < 0.0001$, uncorrected for display purpose). (Right) Metamemory processing areas for recent OLD condition (OLD4). pspd, posterior supraprincipal dimple; ps, principal sulcus; as, arcuate sulcus; aPSPD, metamemory area anteriorly from pspd; mPSPD, metamemory area medially from pspd; SEFa, metamemory area in anterior part of supplementary eye field (SEF). (**D**) Percent signal changes in each cue position of OLD conditions (OLD1–4) and in NEW conditions at bilateral aPSPD and SEFa (square, left; circle, right). ‡$P < 0.001$, *t* test against zero, Bonferroni's correction. Error bar, SEM. (**E**) Intersession correlation between confidence judgment performance [phi coefficient (Φ), *z*-transformed] and fMRI activity (high bet versus low bet, *z*-transformed). *$P < 0.05$, **$P < 0.01$, Bonferroni's correction. Each symbol represents data from each session (square, left; circle, right). (**F**) Correlation coefficients between Φ and fMRI activity [as calculated in (E)] for all metamemory processing areas. *$P < 0.05$, **$P < 0.01$, Bonferroni's correction. PMv, ventral premotor area; PEa/DIP, area PEa/depth of intraparietal area. (**G**) Task-evoked connectivity maps [psychophysiological interaction (PPI) for high bet > low bet] for the seed at left aPSPD in remote OLD condition and for the seed at left SEFa in recent OLD condition ($z > 3.1$, $P < 0.001$, uncorrected for display purpose). IPL, inferior parietal lobule; SPL, superior parietal lobule; ips, intraparietal sulcus.

Downloaded from http://science.sciencemag.org/ on October 27, 2017

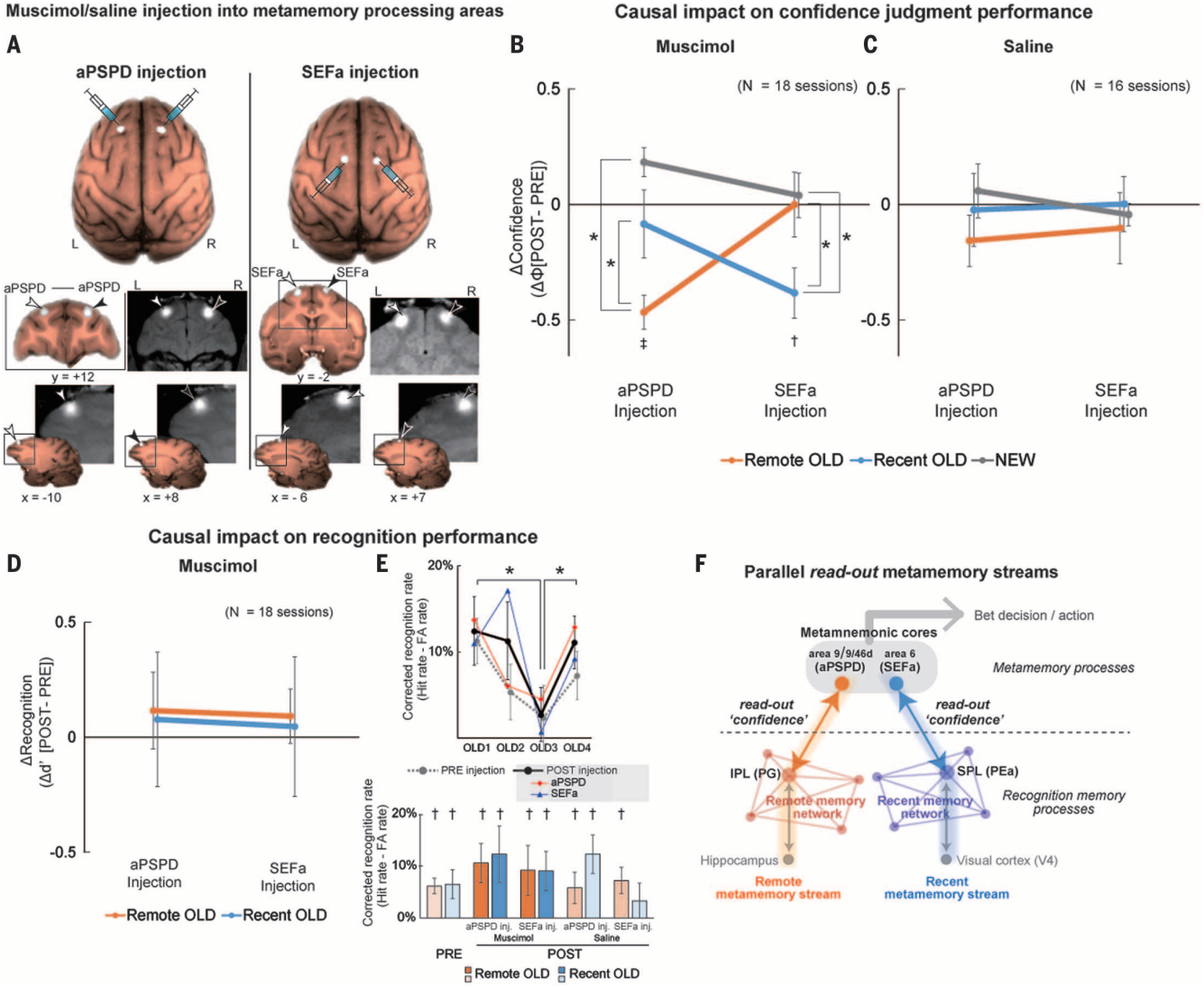

Fig. 4. Double dissociation of causal behavioral impact by reversible inactivation of metamnemonic loci. (**A**) Muscimol or saline was bilaterally injected at aPSPD (left) or SEFa (right). (Top) Gadolinium contrast agent visualized by MRI (white) overlaid on the surface of template brain (copper color). (Bottom) Enlarged view of gadolinium injection sites on coronal and sagittal slices of T1-weighted images. Frame, positions of the enlarged views. (**B**) Performance changes in confidence judgment after muscimol injection in aPSPD (nine sessions) and SEFa (nine sessions). Behavioral effects were evaluated using ΔΦ coefficient [ΔΦ: Φ(POST injection) – Φ(PRE injection)]. *P < 0.05, paired t test, Ryan's correction. †P < 0.05, ‡P < 0.001, t test against zero, Bonferroni's correction. (**C**) Performance change in confidence judgment after saline injection in aPSPD (eight sessions) and SEFa (eight sessions). (**D**) Performance changes in recognition memory after muscimol injection. Behavioral effects were evaluated by Δd' [d'(POST injection) – d'(PRE injection)]. (**E**) (Top) Recognition memory performance before (PRE; dotted light gray) and after (POST; black) injection. Red, aPSPD (POST); blue, SEFa (POST). *P < 0.05 paired t test, in POST injection. (Bottom) Corrected recognition rates (hit rate – false alarm rate) for all conditions in PRE and POST injections. †P < 0.05, t test against zero. No significant difference was found between each POST-injection condition and PRE-injection (t test, P > 0.05, Bonferroni's correction). Error bars in (B) to (E), SEM. (**F**) Proposed parallel metamemory streams. aPSPD is the read-out site of confidence for the remote metamemory stream, whereas SEFa is for the recent metamemory stream. These two streams interact with recognition memory networks for remote and recent memories, respectively.

reward expectation, and reward prediction error) (*5*). However, it is unlikely in the present study for two reasons. First, the memory retrieval period in which we extracted metamemory-related signals is sufficiently separate from the reward delivery period to avoid reward-related effects. We confirmed absence of signal enhancement during memory retrieval period in reward-related areas (ventral tegmental area and amygdala), which were active when wagering (fig. S8, C and D). Second, the almost nonoverlapping distribution of metamemory processing areas between OLD and NEW conditions (Fig. 3, A and B) cannot be explained by reward-related signals, because these signals should be carried equally in both conditions. We also note that the metamemory signals derived from these comparisons could potentially reflect attention during memory retrieval. However, monkeys performed the task without behavioral biases for either "seen" or "not-seen" trial (fig. S2B), and the confidence is measured regardless of trial types (see supplementary text). Moreover, even the fMRI signals in area 9/46v, a central region for covert attention to visual stimuli (*23*, *24*), were differentially modulated by remote and recent memories (fig. S8, A and B), as well as those in aPSPD and SEFa (fig. S4B), all of which suggested that the metamnemonic activities we reported do not covary with the previously reported neuronal activity for attention to visual stimuli (*23*).

Contributions of the mid-dorsolateral prefrontal cortex for both self-ordering task and serial order memory task were reported previously (*25*, *26*).

Downloaded from http://science.sciencemag.org/ on October 27, 2017

Breakthroughs for psychological and behavioral experimental framework on metacognition in animals (*12*, *13*), as well as for whole-brain functional imaging, enabled us to extract neural correlates of metamemory in monkeys, one of which locates at aPSPD around the boundary of anatomically defined area 9 and 9/46d (*3*). Further characterization of aPSPD by both its cognitive functional roles and connections with other brain areas (*27*) would extend our knowledge on this almost uninvestigated area in the dorsal prefrontal cortex (see supplementary text).

It was demonstrated that lateral intraparietal cortex (LIP) neurons in the posterior parietal cortex, which contribute to both visual processing and perceptual decision, also carry information on confidence (*15*). In the present study, inactivation of aPSPD and SEFa caused impairments in metamnemonic judgment without impairing recognition itself; this suggests a role for read-out of confidence on memory in the prefrontal cortex (see supplementary text). A human neuroimaging study based on voxel-based morphometry (*28*) identified a frontopolar cortical area (BA 10) as being a neural correlate of introspection on perceptual decisions. We also found that area 10 in the macaque frontopolar cortex possibly engages in metamnemonic processes for NEW items (see fig. S3B). Despite issues with methodological differences (*29*) and interspecies homology in functioning and cortical structures (*30*), these observations provide a new picture of the frontopolar and/or dorsal prefrontal cortical network as having an integrative role for introspective monitoring in primates.

REFERENCES AND NOTES

1. L. R. Squire, B. Knowlton, G. Musen, *Annu. Rev. Psychol.* **44**, 453–495 (1993).
2. S. Dehaene, *The Cognitive Neuroscience of Consciousness* (MIT Press, 2001).
3. M. Petrides, *Philos. Trans. R. Soc. London B Biol. Sci.* **360**, 781–795 (2005).
4. J. I. Gold, M. N. Shadlen, *Annu. Rev. Neurosci.* **30**, 535–574 (2007).
5. M. F. Rushworth, N. Kolling, J. Sallet, R. B. Mars, *Curr. Opin. Neurobiol.* **22**, 946–955 (2012).
6. Y. Miyashita, *Science* **306**, 435–440 (2004).
7. T. O. Nelson, *Psychol. Learn. Motiv.* **26**, 125–173 (1990).
8. A. P. Shimamura, L. R. Squire, *J. Exp. Psychol. Learn. Mem. Cogn.* **12**, 452–460 (1986).
9. R. Passingham, *Curr. Opin. Neurobiol.* **19**, 6–11 (2009).
10. H. Tomita, M. Ohbayashi, K. Nakahara, I. Hasegawa, Y. Miyashita, *Nature* **401**, 699–703 (1999).
11. W. Vanduffel, Q. Zhu, G. A. Orban, *Neuron* **83**, 533–550 (2014).
12. R. R. Hampton, *Comp. Cogn. Behav. Rev.* **4**, 17–28 (2009).
13. J. D. Smith, W. E. Shields, K. R. Allendoerfer, D. A. Washburn, *J. Exp. Psychol. Gen.* **127**, 227–250 (1998).
14. A. Kepecs, N. Uchida, H. A. Zariwala, Z. F. Mainen, *Nature* **455**, 227–231 (2008).
15. R. Kiani, M. N. Shadlen, *Science* **324**, 759–764 (2009).
16. C. R. Fetsch, R. Kiani, W. T. Newsome, M. N. Shadlen, *Neuron* **83**, 797–804 (2014).
17. P. G. Middlebrooks, M. A. Sommer, *Neuron* **75**, 517–530 (2012).
18. K. Miyamoto *et al*., *Neuron* **77**, 787–799 (2013).
19. K. Miyamoto *et al*., *J. Neurosci.* **34**, 1988–1997 (2014).
20. R. R. Hampton, A. Zivin, E. A. Murray, *Anim. Cogn.* **7**, 239–246 (2004).
21. P. G. Middlebrooks, M. A. Sommer, *J. Exp. Psychol. Learn. Mem. Cogn.* **37**, 325–337 (2011).
22. B. Maniscalco, H. Lau, *Conscious. Cogn.* **21**, 422–430 (2012).
23. N. Caspari, T. Janssens, D. Mantini, R. Vandenberghe, W. Vanduffel, *J. Neurosci.* **35**, 7695–7714 (2015).
24. D. Kaping, M. Vinck, R. M. Hutchison, S. Everling, T. Womelsdorf, *PLOS Biol.* **9**, e1001224 (2011).
25. M. Petrides, *Proc. Biol. Sci.* **246**, 293–298 (1991).
26. M. Petrides, *Proc. Biol. Sci.* **246**, 299–306 (1991).
27. J. Sallet *et al*., *J. Neurosci.* **33**, 12255–12274 (2013).
28. S. M. Fleming, R. S. Weil, Z. Nagy, R. J. Dolan, G. Rees, *Science* **329**, 1541–1543 (2010).
29. S. M. Fleming, J. Ryu, J. G. Golfinos, K. E. Blackmon, *Brain* **137**, 2811–2822 (2014).
30. F. X. Neubert, R. B. Mars, A. G. Thomas, J. Sallet, M. F. Rushworth, *Neuron* **81**, 700–713 (2014).

ACKNOWLEDGMENTS

We thank T. Watanabe and A. Fukuda for technical assistance and S. Konishi, T. Hirabayashi, J. Chikazoe, and T. Watanabe for helpful comments. One Japanese monkey used in this research was provided by NBRP "Japanese Monkeys" through the National BioResource Project of the Ministry of Education, Culture, Sports, Science and Technology (MEXT). This research was supported in part by MEXT and the Japan Society for the Promotion of Science (JSPS) KAKENHI Grants 19002010 and 24220008 to Y.M., 16K18367 to T.O., 26890007 to R.S., 16H01281 to M.T., and, 16K21042 to Y.A., CREST, Japan Science and Technology Agency to Y.M., AMED-CREST, Japan Agency for Medical Research and Development to Y.M., Brain Sciences Project of the Center for Novel Science Initiative, National Institutes of Natural Sciences to M.T. (BS271006), and JSPS Research Fellowships for Young Scientists to K.M. (265926). All data necessary to support this paper's conclusions are available in the supplementary materials. K.M. and Y.M. designed the research; K.M., T.O., R.S., and K.T. collected the data; T.O. and Y.A. developed the setup for fMRI experiments; K.T. developed the experimental tools for microinjection ("injectrode"); K.M., T.O., M.T., and Y.M. analyzed the data; K.M., M.T., and Y.M. wrote the manuscript.

SUPPLEMENTARY MATERIALS

www.sciencemag.org/content/355/6321/188/suppl/DC1
Materials and Methods
Supplementary Text
Figs. S1 to S8
Tables S1 to S4
References (*31*–*55*)

29 September 2016; accepted 14 December 2016
10.1126/science.aal0162

Downloaded from http://science.sciencemag.org/ on October 27, 2017

Science

Causal neural network of metamemory for retrospection in primates

Kentaro Miyamoto, Takahiro Osada, Rieko Setsuie, Masaki Takeda, Keita Tamura, Yusuke Adachi and Yasushi Miyashita

Science **355** (6321), 188-193.
DOI: 10.1126/science.aal0162

Are you aware how well you remember?

Self-monitoring and evaluation of our own memory is a mental process called metamemory. For metamemory, we need access to information about the strength of our own memory traces. The brain structures and neural mechanisms involved in metamemory are completely unknown. Miyamoto *et al.* devised a test paradigm for metamemory in macaques, in which the monkeys judged their own confidence in remembering past experiences. The authors combined this approach with functional brain imaging to reveal the neural substrates of metamemory for retrospection. A specific region in the prefrontal brain was essential for meta mnemonic decision-making. Inactivation of this region caused selective impairment of metamemory, but not of memory itself.

Science, this issue p. 188

ARTICLE TOOLS http://science.sciencemag.org/content/355/6321/188

SUPPLEMENTARY MATERIALS http://science.sciencemag.org/content/suppl/2017/01/11/355.6321.188.DC1

REFERENCES This article cites 51 articles, 17 of which you can access for free
http://science.sciencemag.org/content/355/6321/188#BIBL

PERMISSIONS http://www.sciencemag.org/help/reprints-and-permissions

Use of this article is subject to the Terms of Service

Science (print ISSN 0036-8075; online ISSN 1095-9203) is published by the American Association for the Advancement of Science, 1200 New York Avenue NW, Washington, DC 20005. 2017 © The Authors, some rights reserved; exclusive licensee American Association for the Advancement of Science. No claim to original U.S. Government Works. The title *Science* is a registered trademark of AAAS.

Downloaded from http://science.sciencemag.org/ on October 27, 2017

www.sciencemag.org/content/355/6321/188/suppl/DC1

Supplementary Materials for

Causal neural network of metamemory for retrospection in primates

Kentaro Miyamoto, Takahiro Osada, Rieko Setsuie, Masaki Takeda, Keita Tamura, Yusuke Adachi, Yasushi Miyashita

*Corresponding author. Email: yasushi_miyashita@m.u-tokyo.ac.jp

Published 13 January 2017, *Science* **354**, 188 (2017)
DOI: 10.1126/science.aal0162

This PDF file includes

Materials and Methods
Supplementary Text
Figs. S1 to S8
Tables S1 to S4
References

Materials and Methods

All experimental protocols, animal welfare, and steps for ameliorating suffering were in full compliance with the Guidelines for Proper Conduct of Animal Experiments by the Science Council of Japan, with the University of Tokyo's "Guidelines Regarding Animal Research and Animal-Experimentation Manual," and with the "NIH Guidelines for the Care and Use of Laboratory Animals." The experimental protocol was approved by the University of Tokyo School of Medicine Animal Care and Use Committee (Permission Number, MED: P11-098).

Subjects

Two adult female monkeys (*Macaca fuscata*, monkey E: 7.0 kg, monkey O: 6.5 kg) participated in both functional MRI (fMRI) experiments and behavioral reversible inactivation experiments. Monkeys were housed in standard primate cages in an air-conditioned room under a 12/12-h light-dark cycle. Toys and puzzle feeders were provided for environmental enrichment. Monkeys were given primate food supplemented with fruits and vegetables.

Prior to all experiments, monkeys were trained and adapted to perform behavioral tasks outside and inside the magnet bore of an MRI scanner as described previously (*18, 19, 31-33*). We started the training from the naïve state in one monkey (O), and for the other monkey (E) training started from a well-trained state for a conventional recognition task. For monkey O, it took four months for acquisition of the conventional recognition task. For both monkey O and E, it took five months for acquisition of the metamemory task (learning criteria, phi coefficient > 0 for OLD and NEW conditions over three consecutive days), and three months for acquisition of steady task performance inside the MRI gantry. Functional MRI experiments began when the monkeys were consistently able to perform both recognition memory tasks and confidence judgments regarding their own retrieved memory in the MRI scanner with non-invasive head stabilization (*18, 19, 33*). Before inactivation experiments, a head holder and a recording chamber for microinjection were surgically implanted under aseptic condition into the skull using titanium screws and dental acrylic according to standard protocols (*34, 35*) under sterile conditions. Monkeys were initially sedated with medetomidine (0.03 mg/kg, i.m.) and midazolam (0.3 mg/kg, i.m.), and next they were anesthetized by isoflurane (0.8-1.7 %) throughout the surgery under mechanical ventilation. Surgical treatments were performed after confirming the disappearance of pain reflex. During the anesthesia, blood pressure, heart rate, SpO2 and EtCO2 were continuously monitored to optimize ventilation and gas concentration. Atropine (0.015 mg/kgBW, i.v.) or ephedrine (0.16 mg/kgBW, i.v.) was administered as needed to sustain heart rate and blood pressure. Body temperature was maintained with a heat blanket. Monkeys were given postsurgical analgesics (ketoprofen, 1 mg/kg/day, i.m.) for at least three days, as well as postsurgical prophylactic antibiotics (benzylpenicillin, 20,000 unit/kg/day; ampicillin, 100 mg/kg/day, i.m.; or enrofloxacin, 5mg/kg/day, subcutaneous injection) for one week as described previously (*18*).

Behavioral Tasks

Online behavioral control and reward delivery were implemented in the Presentation platform as described previously (*18, 19*). In a custom-made MRI-compatible monkey chair, each monkey manipulated an optical fiber-based, custom-made three-way joystick with one of its forelimbs (monkey E: right hand, monkey O: left hand) (*18, 19, 33*). In both fMRI and inactivation experiments, monkeys performed the same behavioral task.

Each trial consisted of a Memory stage and a Bet stage, separated by a 4 s inter-stage period (Fig. 1B). In

the Memory stage the animals were required to perform a serial probe recognition task (*36*) as described previously (*18*). In the Bet stage, animals were required to make confidence judgments regarding their decisions during the Memory stage in a post-decision wagering paradigm (*21, 37, 38*): They were required to report, via a wager, whether a correct response had been likely made in the precedent Memory stage. To obtain a reward on any trial, completion of both Memory and Bet stages was required.

Memory stage

Each trial began with the presentation of a fixation point after the monkey pulled the joystick ("Warning", Fig. 1B). The list of four cue items then appeared serially ("Cue 1–4"). Each item was presented at the center of the monitor for 700 ms followed by interstimulus intervals of 500 ms. For the stimuli, 1,000 pictures of natural or artificial objects selected from the HEMERA Photo-Object database were used, which were cropped and presented to the animals at a visual angle of 3.6 × 3.6 degrees. Each picture was presented in only one trial on each experimental day (session). As the same 1,000 pictures were used across sessions, each picture basically appeared at every session. The last list item was followed by a delay period ("Delay") that varied between 3.5 and 5.5 s trial-by-trial. Then, the monkey was presented with two choice stimuli, one test item and one "not seen" symbol (a triangle for monkey E and a cross for monkey O), one each on the right and left side at 3.9 degrees ("Choice"). The assignment of an item and the symbol to the left or right side was randomly selected trial by trial. In half the trials, the test item in the choice period was the same as one of the cue items, and in the other half of trials, the item had not been presented as a cue item. Monkeys were required to respond by moving the joystick in the direction of a test item, if the test item was from the cue item list, or by moving the joystick in the "not seen" symbol direction if it was not from the list. At the Memory stage, they received no performance feedback, or reward delivery. Eye position was monitored at 120 or 240 Hz using an infrared-sensitive CCD camera (*33*). We confirmed that the eye position was within approximately two degrees from the fixation point when each item in the cue list was presented (the deviation of eye position from the fixation point for each item: average, 0.96 deg.; standard deviation, 1.65 deg.; proportion of fixation within two degrees, 85.9%). If the monkey released the joystick before the choice period, or failed to respond to either choice stimulus within the time limit of 6 s, the trial was aborted, and the next trial began after a 4-s inter-trial interval.

Bet stage

A fixation point reappeared after the monkey pulled the joystick to initiate the Bet stage ("Warning", Fig. 1B). After a random interval of 0.5–2.5 s, two bet targets appeared: a pink "high-bet" target and a green "low-bet" target (for Monkey E; color assignments were reversed for Monkey O). The assignment of high-bet and low-bet targets to the left or right side was randomly selected for each trial. Monkeys reported their bet by moving the joystick in the direction of one of the two bet targets. At the end of each trial, a reward was delivered, the amount of which was based on how appropriate the bets were relative to memory performance during the Memory stage. If the monkeys correctly answered in the Memory stage and bet high, they earned the maximum reward (monkey E: 0.8 mL, monkey O: 1.1 mL). If the monkeys made an incorrect decision in the Memory stage and bet high, they received no reward and a 10 s time-out. Betting low earned a sure but minimal reward (monkey E: 0.6 mL, monkey O: 0.6 mL for correct decisions; monkey E: 0.5 mL, monkey O: 0.4 mL for incorrect decisions). The reward schedule was determined based

on previous studies on perceptual metacognition (*21, 38*). In the training of metamemory task, the reward schedule was adjusted so that each animal chose high-bet and low-bet options almost equivalently and stably. Then the schedule was fixed and consistently used in the following experiments. Monkeys could optimize the total amount of received reward by placing high bets following a correct decision in the precedent Memory stage and low bets after an incorrect decision (Fig. 1B). If monkeys released the joystick before making a bet, the trial was immediately aborted. The next trial began after a 4-s inter-trial interval.

Imaging data acquisition

Whole-brain functional mapping was conducted during performance of the metamemory task in supine position. Functional images were acquired in a 4.7-T MRI scanner with 100 mT/m actively shielded gradient coils and a transceiver saddle RF coil, as described previously (*18, 19, 33*). In each session, functional data were acquired using a gradient-echo echo-planar imaging (EPI) sequence (1-shot, TR = 2.5 s, TE = 20 ms, 1.25 × 1.5 mm^2 in-plane resolution, 64 × 96 matrix, slice thickness = 1.5 mm with inter-slice gap = 0.2 mm, 30 horizontal slices covering the whole brain).

In separate sessions, under propofol anesthesia (5–10 mg/kg/h, i.v.), high-resolution T1-weighted structural images of the monkey brains were obtained using the 3D-MDEFT sequence (0.5 mm isotropic). High-resolution EPI (32-shot, TR = 3 s, TE = 20 ms, 0.625 × 0.75 mm^2 in-plane resolution, 128 × 192 matrix, slice thickness = 0.75 mm with inter-slice gap = 0.13 mm, 54 horizontal slices covering the whole brain) were also acquired to serve as the template images for spatial normalization (see below). For acquisition of structural images to display injected sites by gadolinium contrast medium (Fig. 4A; see below for more details), we scanned T1-weighted structural images using the RARE sequences (TR = 1.0 s, TE = 11.4 ms, 0.4 × 0.4 mm^2 in-plane resolution, 256 × 256 matrix, slice thickness = 1.0 mm, 26 coronal slices or 30 sagittal slices covering the injected sites).

Targeted reversible inactivation and behavioral test

Muscimol microinjection

We microinjected a GABA-A receptor agonist (muscimol) into the metamemory processing areas in the aPSPD or SEFa, which we identified by fMRI experiment, in order to evaluate the causal contribution of these areas to metacognitive behavior. We administered microinjections 1) to the bilateral target sites in the aPSPD or 2) to the bilateral target sites in the SEFa in separate sessions. We used an injection-electrode (injectrode) specifically developed for microinjection in non-human primates. To minimize the tissue damage, the coordinates of microinjection were changed across experimental sessions within 3 mm from the coordinates of activation peaks in each hemisphere localized in the fMRI experiments in each monkey (see *Imaging data* in Data Analysis below). We inserted the injectrode while recording single-/multi-unit activities. By the online unit activity monitoring, in every session we identified the cortical surfaces of the target sites and placed the injectrodes' tip at a depth of 1.0 mm from the cortical surface, corresponding to the grey matter of the target cortical sites. We injected muscimol (3.33 mg/mL dissolved in saline, 1.5 μL/site) at a speed of 2 nL/1.2 s in ten minutes after reaching the targeted depth. We confirmed that spiking activities was diminished following the microinjection. Ten minutes after completion of injection, we removed the injectrodes.

Saline microinjection

As a control experiment against muscimol injection, we conducted saline microinjection. In a similar way to the muscimol experiments, we administered microinjections to the bilateral target sites in 1) the aPSPD or 2) the SEFa in separate sessions, using the injectrode. We performed saline microinjection following the same protocol using the same apparatus as muscimol microinjection. The coordinates of injection sites, depth of injection site from the identified cortical surface (1.0 mm), injection volume (1.5 μL), and injection speed (2 nL/1.2 s) were the same as in the muscimol experiments.

Behavioral test schedule

In each experimental session, monkeys first performed a standard serial probe recognition task (Memory stage only) for warm-up (15–20 trials), and then they performed the metamemory task (typically 60 trials; PRE). After this PRE-injection behavioral test, we conducted microinjection of muscimol or saline (see above). Monkeys performed the same metamemory task (typically 60 trials; POST) and a standard serial probe recognition task (15–40 trials), after 30–90 minutes of completion of microinjection. On separate days, we performed non-injection experiments, in which the time schedule was approximately the same as the injection experiments (see *Behavioral data* in Data Analysis below). We performed the injection experiments in the order of muscimol injection, non-injection, and saline injection. Non-injection experiments were always conducted at least 2 days after muscimol injection to ensure the absence of muscimol after-effects during these sessions. We administered muscimol at least two days following the saline injection. We performed a total of 18 muscimol injection sessions (nine sessions each for aPSPD and SEFa [five from monkey E and four from monkey O]), 16 saline injection sessions (eight sessions each for aPSPD and SEFa [four from each monkey E and O]), and 26 non-injection sessions (14 sessions from monkey E and 12 sessions from monkey O).

Gadolinium contrast medium injection

To confirm that muscimol/saline was precisely delivered to the targeted sites, we bilaterally injected gadolinium contrast medium (MRI contrast agent) to the same sites in the aPSPD or SEFa in separate sessions, instead of muscimol or saline. The monkeys were anaesthetized (by propofol) in order to stabilize their head for high-quality structural MRI scans. We performed microinjection following the same protocol with the same apparatus as muscimol/saline microinjections. The coordinates of injection sites and depth of injection site from the identified cortical surface (1.0 mm) were the same as in the muscimol experiments. Gadolinium contrast medium (25 mM dissolved in saline, 2.0 μL/site) was injected at a speed of 2 nL/1.2 s. Immediately after removal of injectrodes, we conducted structural T1-weighted MRI scans (RARE) (Fig. 4A).

Data analysis

Behavioral data

Recognition memory performance was evaluated by both "corrected recognition rate" (Hit rate – False Alarm rate) (*39*) and *d'* index of type-I signal detection theory (*40*). Metamnemonic performance of monkeys was evaluated both

by phi coefficient (Φ), a contingency-table-based correlational index (*21, 37*) and by meta-*d'*, an index based on type-II signal detection theory (*22*). The Φ index was calculated according to the following formula using the number of trials classified in each case [*n*(case)]:

$$\text{phi coefficient } (\Phi) = \frac{n(Correct\ \ High)\times n(Incorrect\ \ Low) - n(Correct\ \ Low)\times n(Incorrect\ \ High)}{\sqrt{n(Correct)\times n(Incorrect)\times n(High)\times n(Low)}}$$

This Φ index (Fig. 2B) evaluates how optimally each trial was assigned for high- or low-bet in the Bet stage, based on performance in the preceding Memory stage. We calculated the index for each session in each memory condition (OLD, NEW, Remote OLD, and Recent OLD). In addition, the meta-*d'* index (Fig. S1D) was calculated using Type 2 SDT toolbox on Matlab developed by Maniscalco and Lau (*22*), which has been widely used for evaluation of metacognitive skills (*29, 41*). We analyzed and summarized behavioral data acquired outside an MRI scanner before behavioral reversible inactivation experiments (Fig. 2). We confirmed that monkeys performed this task similarly during the fMRI scanning sessions (Fig. 3) and during the PRE injection of behavioral reversible inactivation (Fig. 4). To evaluate causal metamnemonic impairment in inactivation experiments, we used the following formula: ΔΦ = Φ[POST injection] – Φ[PRE injection] (Fig. 4B). The ΔΦ index was calculated separately for Remote OLD ($\Delta\Phi^{Remote}$), Recent OLD ($\Delta\Phi^{Recent}$), and New ($\Delta\Phi^{New}$) conditions. We subtracted the average ΔΦ in non-injection experiments (Monkey E, Remote OLD, +0.07; Recent OLD, -0.20; NEW, -0.05; Monkey O, Remote OLD, +0.01; Recent OLD, -0.04; NEW, 0.04) from this index to remove effects of response bias. Even when injection data were analyzed without subtracting the average ΔΦ in non-injection experiments, the results were reproduced: the interaction between Injection site (aPSPD, SEFa) and memory condition (Remote OLD, Recent OLD, NEW) for the behavioral impacts on confidence judgement after muscimol injection was significant ($F_{2,28}$ = 5.95, p = 0.0070). We also evaluated the degree of causal metamnemonic impairment using a signal-detection theory-based metacognitive efficiency index Δ(meta-*d'* – *d'*) (*22, 29*) (Fig. S6C). To evaluate causal recognition impairments, we used the following formula: Δd' = d'[POST injection] – d'[PRE injection] (Fig. 4D).

Imaging data

We conducted preprocessing and whole-brain analysis of fMRI data with SPM8 (http://www.fil.ion.ucl.ac.uk/spm) as described previously (*18, 19, 31-33*). Functional images were realigned, corrected for slice timing, spatially normalized to the template image with interpolation to a 1 × 1 × 1-mm^3 space, and smoothed with a Gaussian kernel (3 mm full-width at half-maximum). The template image was constructed from the high-resolution EPI of Monkey O by co-registering it to Monkey O's anatomical template MDEFT image and arranged in the bicommissural space in which the origin was placed at the anterior commissure (*18, 31-33*).

We performed a voxel-wise GLM analysis implemented in SPM. These analyses included the following predictors: (1–8) the choice onsets during the Memory stage separately for eight categories (four memory conditions [Hit, Correct Rejection (CR), Miss, False Alarm (FA)] × two bet conditions [high-bet, low-bet]); (9–16) the bet onsets during the Bet stage separately for the same eight categories; and (17) the cue-item onsets. These events were modeled as delta functions convolved with the canonical hemodynamic response function and its temporal and dispersion derivatives. The six parameters of head motion derived from realignment were also included in the model as

covariates of no interest. The group analysis of the data from the two monkeys (monkey E, 1,049 trials, 84 runs; monkey O, 1,198 trials, 49 runs) was conducted using a fixed-effect model. Metamemory processing areas were identified by the group analysis map that compared BOLD signals for choice onset during the Memory stage between high-bet and low-bet conditions. We localized metamemory processing areas separately for OLD condition (Fig. 3A, Table S1A) and NEW condition (Fig. 3B, Table S1B). The coordinates of the activation peaks at the threshold of $p < 0.05$ with family-wise error (FWE) correction across the whole brain volume were listed in Table S1. If a homotopic activation peak (*32, 33, 42*) in the contralateral hemisphere (significant at $p < 0.05$ uncorrected) locates within the 6 mm-radius from the symmetrical (x-flipped) points of one peak identified above, the peak was also included in the table. The peaks were labeled by referring to the atlas of Paxinos et al. (*43*). To examine neural activity of metamemory for different memory processes (see Fig. S1B), we then separated predictors for OLD conditions in the voxel-wise GLM analysis into Hit for the initial three items (Remote OLD condition) and Hit for the last items (Recent OLD condition), and localized metamemory processing areas separately (Fig. 3C and Table S2). Following the same procedure for OLD and NEW conditions, the coordinates of activation peaks were listed in Table S2. We also evaluated inter-subject reproducibility of the results by conducting the same analyses for individual monkeys separately (Fig. S4A, S5, Table S4). Based on this analysis, conjunction maps (conjunction null, $p < 0.01$, uncorrected for each monkey) of metamemory processing areas across monkeys were generated (*18, 44*) (Fig. S4C).

To identify the locus in which activity predicts metamnemonic performance, we calculated correlation coefficients between confidence judgment performance (Φ) and fMRI activity in metamemory processing areas in each hemisphere across experimental sessions (Fig. 3D–F). For reliable evaluation of Φ index, sessions with at least seven trials were included for each trial condition (Remote OLD, monkey E, 13 sessions, monkey O, 9 sessions; Recent OLD, monkey E, 11 sessions, monkey O, 9 sessions; NEW monkey E, 14 sessions, monkey O, 9 sessions). To examine neural activity predicted by Φ index of each monkey, fMRI activity was extracted based on analysis for individual monkeys as follows: we identified the nearest peak ($p < 0.05$) from the group coordinates listed in Table S2 in each monkey and defined the area within 2-mm of each peak as a region of interest (ROI); if no significant peak was found within 6 mm around the group coordinate, the group coordinate was substituted for the nearest peak; the average of signal across all voxels in each ROI was used for the following analyses. Metamnemonic performance and fMRI activity were z-transformed (across sessions for each monkey) before the correlation coefficient was calculated.

To examine task-evoked connectivity between aPSPD/SEFa and other cortical areas in response to metamemory processes during memory retrieval, we conducted psychophysiological interaction (PPI) analysis (*45*). We calculated 1) PPI in high-bet vs. low-bet responses for the Remote OLD condition by setting the left or right aPSPD as the seed and 2) PPI in high-bet vs. low-bet responses for the Recent OLD condition by setting the left or right SEFa as the seed, respectively. In each hemisphere of each monkey, the coordinate of the seed (radius, 2 mm) corresponded to that of the muscimol injection site showing the largest metamnemonic impairment ($\Delta\Phi$). Significant peaks of PPI at a cluster-level of $p < 0.05$, corrected by false discovery rate (FDR) across the whole brain (*46*) (thresholding criteria, $z > 2.3$) (*47, 48*), were listed in Table S3. If the PPI was significant at $p < 0.05$ corrected by family-wise error (FWE) for small volume in the contralateral region for each significant peak (within 2 mm of the

coordinate of activation peak), the coordinate of the contralateral peak was also included in the table. The location of each cluster were labeled by referring to the atlas of Paxinos et al. (*43*).

Statistics

We corrected p-values for multiple comparison when necessary. The methods for multiple comparison were mentioned when used. For identification of metamemory processing areas, we applied FWE correction across the whole-brain volume; therefore, fMRI results were not overestimated. Error bars in the figures depict standard errors of the mean (s.e.m.). No statistical methods were used to predetermine sample size. However, our sample size for numbers of animals, behavioral sessions, and fMRI runs/volumes were similar to those reported in previous publications (*18, 19, 31-33, 49, 50*).

Supplementary Text

Anatomy and functinal connectivity of aPSPD

The posterior supraprincipal dimple, immediately anteriorly to which aPSPD is located, is around the boundary between areas 9, 9/46d, and area 8 (see the middle panel of Fig. 3C) in the prefrontal cortex (*3*). Petrides (*3*) indicated that the border between area 9 and area 9/46d almost corresponds to the extended line of superior branch of arcuate sulcus, and that the lateral prefrontal surface immediately anterior to the posterior supraprincipal dimple is classified as area 9. In light of the cytoarchitectonic map by Petrides (*3*), aPSPD we identified by the fMRI experiments locates dominantly on area 9, even though some parts of it may locate on area 9/46d. The cognitive functions related to aPSPD have not yet been investigated before. Recently, Sallet et al. (*27*) investigated resting-state functional connectivity in monkeys and demonstrated that the connectvity pattens with other brain sites were different between areas 9 and 9/46d: area 9/46d had strong resting-state functional connectivity with the inferior parietal lobule, whereas area 9 did not have such a strong connection. In Sallet et al. (*27*), the ROI of area 9 was set at the medial wall. On the other hand, aPSPD identified in the present study locates on the lateral prefrontal surface around area 9. The prefrontal cortex is known as an area where individual structural differences are more prominent than in other cortical areas, even in monkeys (*51*). Invesigations on resting-state functional connectivity patterns with other brain sites for aPSPD will characterize the functional positioning of aPSPD in the whole-brain network, in comparison with sorrounding areas in the dorsal prefrontal cortex, such as the ROIs of area 9 and 9/46d by Sallet et al. (*27*).

Functional roles of mid-dorsolateral prefrontal cortex for memory monitoring

The roles of the mid-dorsolateral prefrontal cortex for monitoring the contents of memory was addressed by Petrides (*3*). The extent of the mid-dorsolateral prefrontal cortex spans across areas 9/46d, 9, and 46. Indeed, Petrides (*25, 26*) reported that a lesion in the mid-dorsolateral prefrontal cortex induced not only impairments of memory assessment in a self-ordering task, but also impairments of memory assessment for externally ordered items at the middle position in a serial order memory task. However, it is unknown if the responsible areas for self-ordering task and serial order memory task are segregated or overlapped in the mid-dorsolateral prefrontal cortex.

Recent development of psychological/behavioral framework for experimentation of metacognitive skills in animals (*12, 13*) enabled us to extract neural correlates of metamemory in monkeys, which is separated from memory execution itself. In the present study, by whole-brain searches with fMRI mapping (*11, 52*), we found that one of the responsible sites for metamnemonic judgements, but not for memory execution, is focally localized at aPSPD within the mid-dorsolateral prefrontal cortex. Thus, our present findings would extend the view of responsible functions in the mid-dorsolateral prefrontal cortex.

Functinal roles of the supplementary eye field

The supplementary eye field (SEF), which almost corresponds to rostral dorsal premotor cortex (F7) in area 6, was originally defined as an area, of which electric microstimulation triggers eye movement in macaques (*53*). Therefore, SEF has been historically investigated as an area that supports or supervises eye movement control. Recently, several lines of evidence have accumulated for SEF functions suggesting other than eye movement control. For example,

SEF cells of monkeys also came to be known to code familiarized stimuli in a non-spatial manner (*54*). In particular, Middlebrooks and Sommer (*17*) suggested that SEF cells relate to perceptual metacognitive control. In the present study, it was causally demonstrated that SEFa is eccential for metamnemonic judgment on recent memory. Taken together, these findings expand our knowledge on SEF in that it plays the role not only to supervise oculomotor movements but also to supervise our own perceptual/memorial judgement.

Behavioral task design using 'seen' picture and 'not seen' symbol

In the present study, we adopted the behavioral task design using the 'seen' picture and 'not seen' symbols. This design may possibly bring the difference in covert attention between high- and low-bet trials. The difference would be minimized if abstract 'seen' and 'non-seen' symbols next to pictures were used in each trial, as similarly in the authors' previous studies (*18, 19*). This task design, however, required additional cognitive demands for monkeys to assign 'seen'/'non-seen' trial to 'seen'/'non-seen' symbol. In the present study, because we added Bet stage which requires assignment of 'high-bet'/'low-bet' trial with 'high-bet'/'low-bet' coloured symbol, we simplified the task design so as to relieve task demands on monkeys. In theory, if monkeys did not have biases for either seen picture or non-seen symbol, attention will not be a problem for measured fMRI signals because the confidence of the animals is measured regardless of trial type. To examine if this premise is the case for the present study, we evaluated the possible bias by calculating the interaction (seen/non-seen item [answer] × high/low bet) (Fig. S2B). We found that statistical significant interaction was not observed in either monkey (All trials, Monkey E, $F_{1,15} = 1.28$, $p = 0.27$, Monkey O, $F_{1,15} = 0.031$, $p = 0.86$; Correct trials, Monkey E, $F_{1,15} = 0.93$ $p = 0.34$, Monkey O, $F_{1,15} = 0.67$, $p = 0.42$). These results support that differences in fMRI signals during Memory stage would not originate from the experimental design using a seen picture and non-seen symbol.

fMRI signals in prefrontal areas with attentional modulations

For attentional modulations in macaque prefrontal cortex, Caspari et al. (*23*) conducted a whole-brain fMRI mapping in behaving monkeys and reported that area 46 and SEF/F7 were included in the regions activated in correlation with covert attention. By single-unit recordings, Kaping et al. (*24*) reported that neurons in VMPFC and LPFC increased spiking activities in response to covert attention. In the present study, for aPSPD and SEFa in the dorsal prefrontal cortex, fMRI results demonstrated a double dissociation in contributions to metamnemonic judgment (interaction between cue position [Cue 1,2,3,4] and areas [aPSPD, SEFa], $F_{3,6} = 5.40$, $p = 0.038$): aPSPD and SEFa are selectively activated for metamnemonic judgements on remote (Cue 1–3) and recent (Cue 4) items, respectively. Both Caspari et al. (*23*) and Kaping et al. (*24*) suggest that area 46/DLPFC is a central area related to covert attention. Thus, we additionally examined whether fMRI activity of area 9/46v was explained by covert attention. We found that the fMRI activity in area 9/46v changes depending on cue item positions (main effect of cue position [Cue 1,2,3,4], $F_{3,6} = 8.64$, $p = 0.013$; interaction between cue position and monkey, $F_{3,6} = 4.03$, $p = 0.068$): metamemory-related activity for remote items is significantly larger than that for recent items (Cue 1 > Cue 4, Cue 2 > Cue 4, Cue 3 > Cue 4, post-hoc t-test, $p < 0.05$, Bonferroni-corrected; Cue 1, 2, 3, t-test against baseline, all $p < 0.05$, Bonferroni-corrected). These fMRI results suggest that the metamnemonic activities we reported do not covary with the previously reported neuronal activity for attention to visual stimuli; therefore, the fMRI activity in aPSPD, SEFa, and 9/46v cannot be

interpreted solely by attention. (Fig. S8A–B) .

Loci of metacognition in prefrontal and parietal cortices

Kiani and Shadlen (*15*) demonstrated that lateral intraparietal area (LIP) neurons in the posterior parietal cortex, which is a locus for both visual processing and perceptual decision making, also carry information on confidence. On the other hand, we found that the two prefrontal loci (aPSPD and SEFa), which is not resonsible for memory execution process itself, are causally essential for read-out of confidence on memory. One of the differences between these two studies may originate from the differences in roles between frontal and parietal cortices, which are relatively related to top-down and bottom-up information processes within a whole-brain network, respectively. Alternatively, the difference may originate from what the metacognitive process monitors: memory or perception. Further investigations on fronto-parietal interaction in both memory and perception during metacognitive judgment are required to reveal the full picture of the whole-brain network for metacognition.

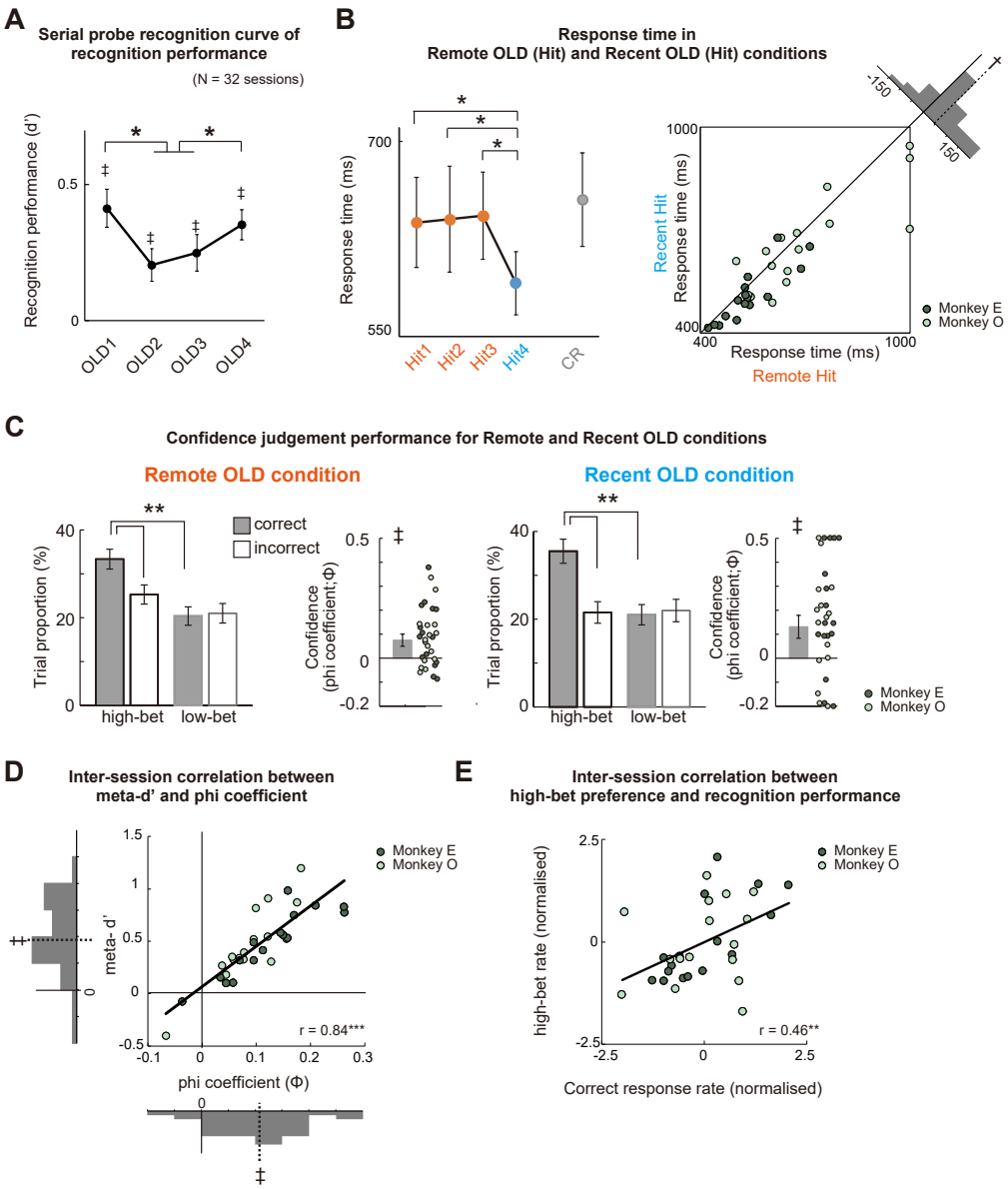
A
Serial probe recognition curve of recognition performance
(N = 32 sessions)
Recognition performance (d')
OLD1
OLD2
OLD3
OLD4
B
Response time in Remote OLD (Hit) and Recent OLD (Hit) conditions
Response time (ms)
Hit1
Hit2
Hit3
Hit4
CR
Recent Hit
Response time (ms)
Remote Hit
Monkey E
Monkey O
C
Confidence judgement performance for Remote and Recent OLD conditions
Remote OLD condition
Recent OLD condition
correct
incorrect
Trial proportion (%)
high-bet
low-bet
Confidence (phi coefficient:Φ)
D
Inter-session correlation between meta-d' and phi coefficient
meta- d'
phi coefficient (Φ)
r = 0.84***
E
Inter-session correlation between high-bet preference and recognition performance
high-bet rate (normalised)
Correct response rate (normalised)
r = 0.46**

Figure S1

Fig. S1. Further evidence for behavioral performance in the metamemory task. (**A**) A serial position curve of recognition performance with significant primacy and recency effects evaluated by *d'* of signal detection theory. *p < 0.05, paired *t*-test, Bonferroni's correction. ‡p < 0.001, *t*-test against zero, Bonferroni's correction. (**B**) Left panel, response latency for each cue position in Correct OLD (Hit1–4) and Correct NEW conditions (Correct rejection [CR]). *p < 0.05, paired *t*-test, Holm's correction. Right panel, relationship of response time between Remote Hit (Hit1–3) and Recent Hit (Hit 4). Histograms show distribution of session-by-session difference. †p = 0.0053, paired *t*-test. (**C**) Confidence judgment performance evaluated by trial proportion and phi-coefficient (Φ). **p < 0.01, paired *t*-test, Bonferroni's correction. ‡p < 0.001, *t*-test against zero. (**D**) Confidence judgment evaluated by meta-*d'* of type-II signal detection theory and by contingency-table-based phi-coefficient. Histogram shows the distribution of session-by-session values. Dotted line denotes mean. ‡p < 0.001, *t*-test against zero. Both meta-*d'* and phi-coefficient were significantly correlated with one another (r = 0.84, ***p = 1.0×10^{-9}). (**E**) Inter-session correlation between high-bet preference and recognition performance (r = 0.46, **p = 0.0077). Each circle in **B**–**E** represents a single session (N = 32). Color of the circles depict data from each monkey. Error bars denote s.e.m.

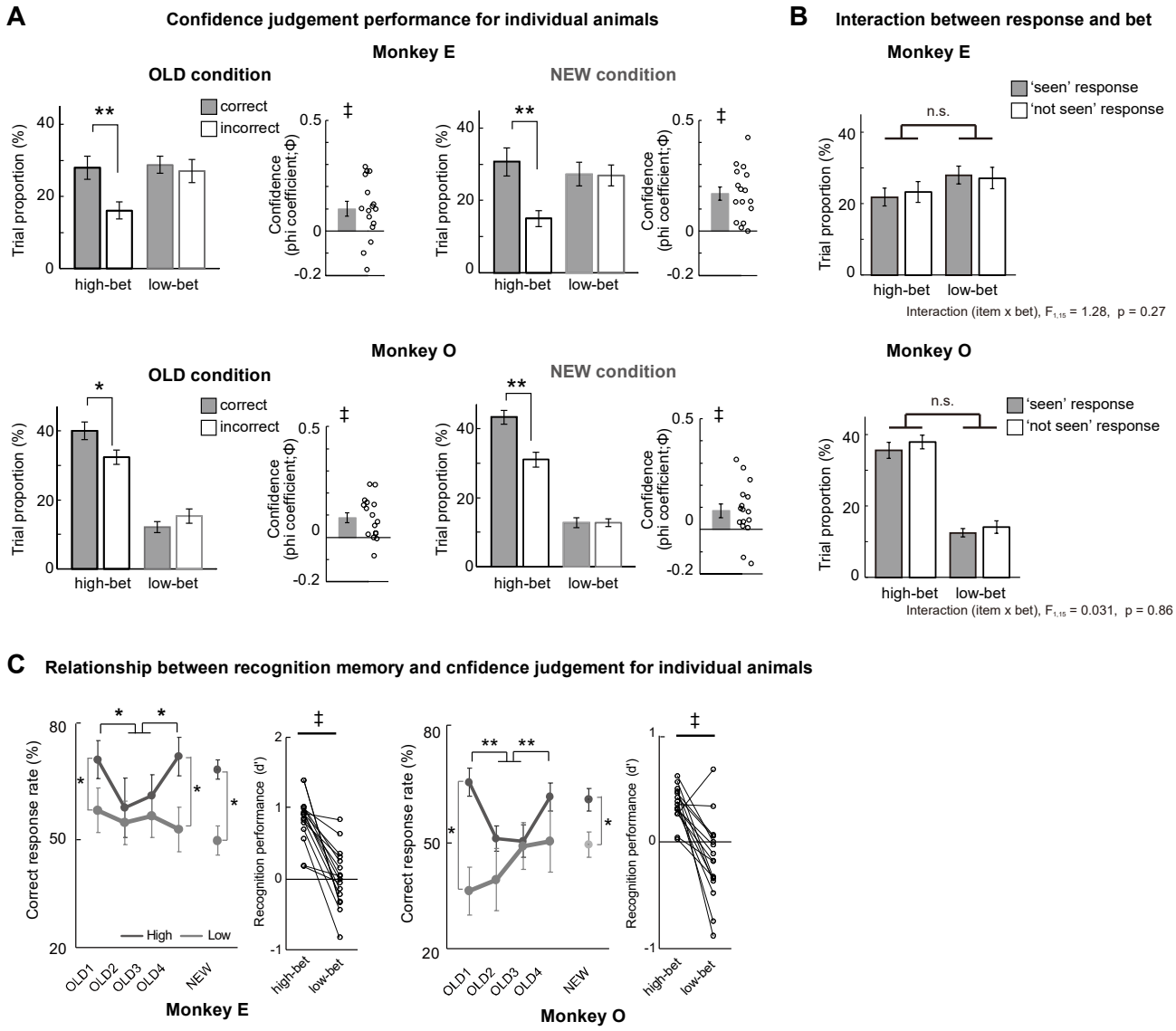
A
Confidence judgement performance for individual animals
Monkey E
OLD condition
NEW condition
correct
incorrect
Trial proportion (%)
Confidence (phi coefficient;Φ)
high-bet
low-bet
Monkey O
B
Interaction between response and bet
'seen' response
'not seen' response
n.s.
Interaction (item x bet), F1,15 = 1.28, p = 0.27
Interaction (item x bet), F1,15 = 0.031, p = 0.86
C
Relationship between recognition memory and cnfidence judgement for individual animals
Correct response rate (%)
Recognition performance (d')
High
Low
OLD1
OLD2
OLD3
OLD4
NEW

Figure S2

Fig. S2. Consistency in confidence judgment performance across subjects. (**A**) Confidence judgment performance evaluated by trial proportion and phi-coefficient (Φ) in individual animals (upper, monkey E, N = 16 sessions; lower, monkey O, N = 16 sessions). *p < 0.05, **p < 0.01, paired *t*-test (Bonferroni's correction). ‡p < 0.001, *t*-test against zero. Configurations are the same as in Fig. 2B. (**B**) Proportion of trials classified by monkey's response. The interaction ('seen'/'non-seen'× high-/low-bet) was not statistically significant for each monkey (All correct and incorrect trials, Monkey E, $F_{1,15} = 1.28$, p = 0.27, Monkey O, $F_{1,15} = 0.031$, p = 0.86; see panel (**A**) for only correct trials, Monkey E, $F_{1,15} = 0.93$, p = 0.34, Monkey O, $F_{1,15} = 0.67$, p = 0.42). (**C**) Recognition performance in high-bet (dark grey) and low-bet (light grey) trials in individual animals. *p < 0.05, **p < 0.01, ***p < 0.001, paired *t*-test, Bonferroni's correction. ‡p < 0.001, paired *t*-test. Configurations are the same as in Fig. 2C.

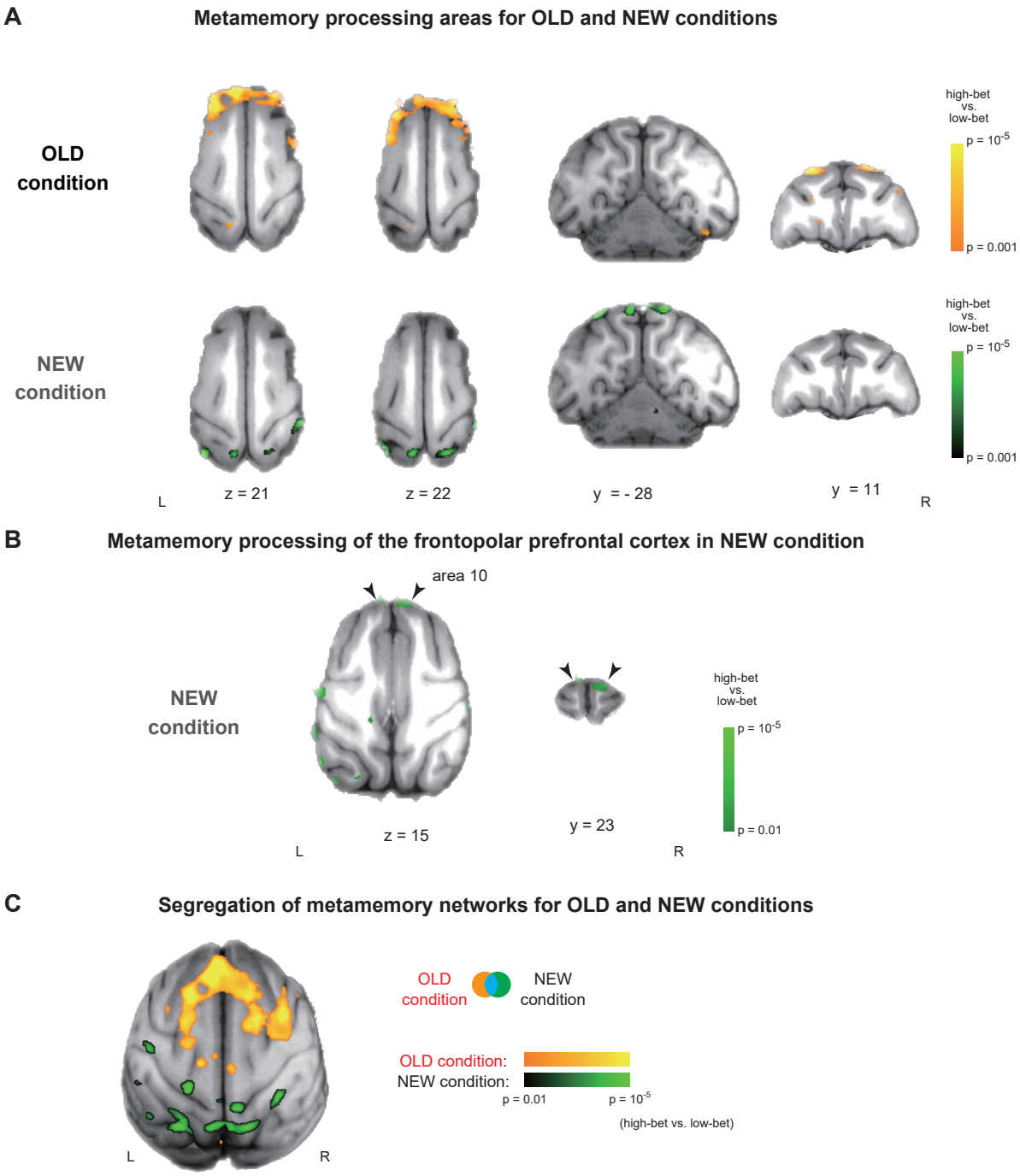
A
Metamemory processing areas for OLD and NEW conditions
OLD condition
NEW condition
high-bet vs. low-bet
p = 10-5
p = 0.001
L
z = 21
z = 22
y = - 28
y = 11
R
B
Metamemory processing of the frontopolar prefrontal cortex in NEW condition
area 10
NEW condition
z = 15
y = 23
p = 0.01
C
Segregation of metamemory networks for OLD and NEW conditions
OLD condition
NEW condition
OLD condition:
NEW condition:
p = 0.01
(high-bet vs. low-bet)

Figure S3

Fig. S3. Metamemory processing areas for OLD and NEW conditions. (**A**) Metamemory processing areas on horizontal (left) and coronal slices (right) shown separately for OLD (upper) and NEW (lower) conditions. $z > 3.1$, $p < 0.001$, uncorrected for display purpose. See Table S1. (**B**) Metamemory processing in the frontopolar prefrontal cortex (area 10) in NEW condition. $z > 2.3$, $p < 0.01$, uncorrected for display purpose. Bilateral regions in the area 10 were activated, even though it does not satisfy the statistical criteria for multiple comparisons (left area 10, [x, y, z] = [–4, 21, 18], $z = 3.13$, $p < 0.001$, uncorrected; right area 10, [x, y, z] = [3, 24, 15], $z = 3.00$, $p = 0.001$, uncorrected). (**C**) Overlap of metamemory processing areas for OLD and NEW conditions (see also Fig. 3A, B). $z > 2.3$, $p < 0.01$, uncorrected for display purpose. The overlap between these two conditions is marginal.

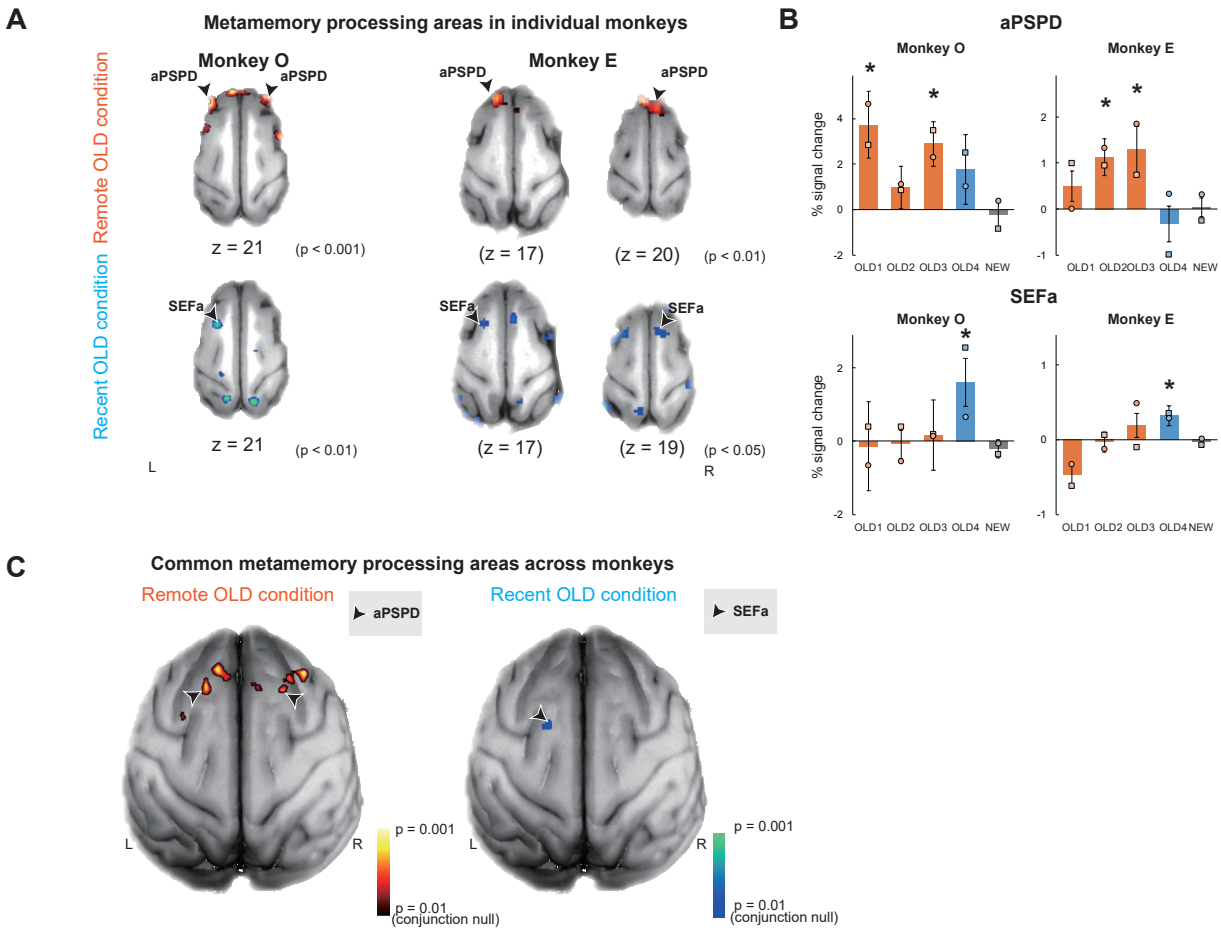
A
Metamemory processing areas in individual monkeys
Recent OLD condition
Remote OLD condition
Monkey O
Monkey E
aPSPD
aPSPD
aPSPD
aPSPD
z = 21
(p < 0.001)
(z = 17)
(z = 20)
(p < 0.01)
SEFa
SEFa
SEFa
SEFa
z = 21
(p < 0.01)
(z = 17)
(z = 19)
(p < 0.05)
L
R
B
aPSPD
Monkey O
Monkey E
% signal change
OLD1 OLD2 OLD3 OLD4 NEW
SEFa
Monkey O
Monkey E
% signal change
OLD1 OLD2 OLD3 OLD4 NEW
C
Common metamemory processing areas across monkeys
Remote OLD condition
aPSPD
Recent OLD condition
SEFa
L
R
p = 0.001
p = 0.01
(conjunction null)
L
R
p = 0.001
p = 0.01
(conjunction null)

Figure S4

Fig. S4. Consistency of metamemory processing areas across subjects. (**A**) Metamemory processing areas for Remote OLD and Recent OLD conditions in individual animals thresholded for display purpose ($z > 3.1$ [$p < 0.001$, uncorrected], $z > 2.3$ [$p < 0.01$, uncorrected], or $z > 1.65$ [$p < 0.05$, uncorrected], as indicated in each panel). Arrows in Remote OLD and Recent OLD conditions represent metamemory processing areas localized in the aPSPD and in SEFa, respectively. Activated areas are overlaid on the 3D brain volume of each monkey. (**B**) Percent signal changes in Remote OLD (OLD 1–3) and Recent OLD (OLD 4) conditions for aPSPD and SEFa (within 2 mm from the activation peaks in individual monkeys; see Table S4). Square, left area, circle, right area. This dissociation was reflected in the significance of interaction in ANOVA (interaction between cue position and areas, $F_{3,6} = 5.40$, $p = 0.038$). *$p < 0.05$, **$p < 0.01$, *t*-test against zero, Bonferroni's correction. Error bars denote s.e.m. (**C**) Common activation map of metamemory processing areas by conjunction analysis (Conjunction null hypothesis (*18, 44*); $t > 2.3$, $p < 0.01$, uncorrected in each monkey). See Materials and Methods in detail.

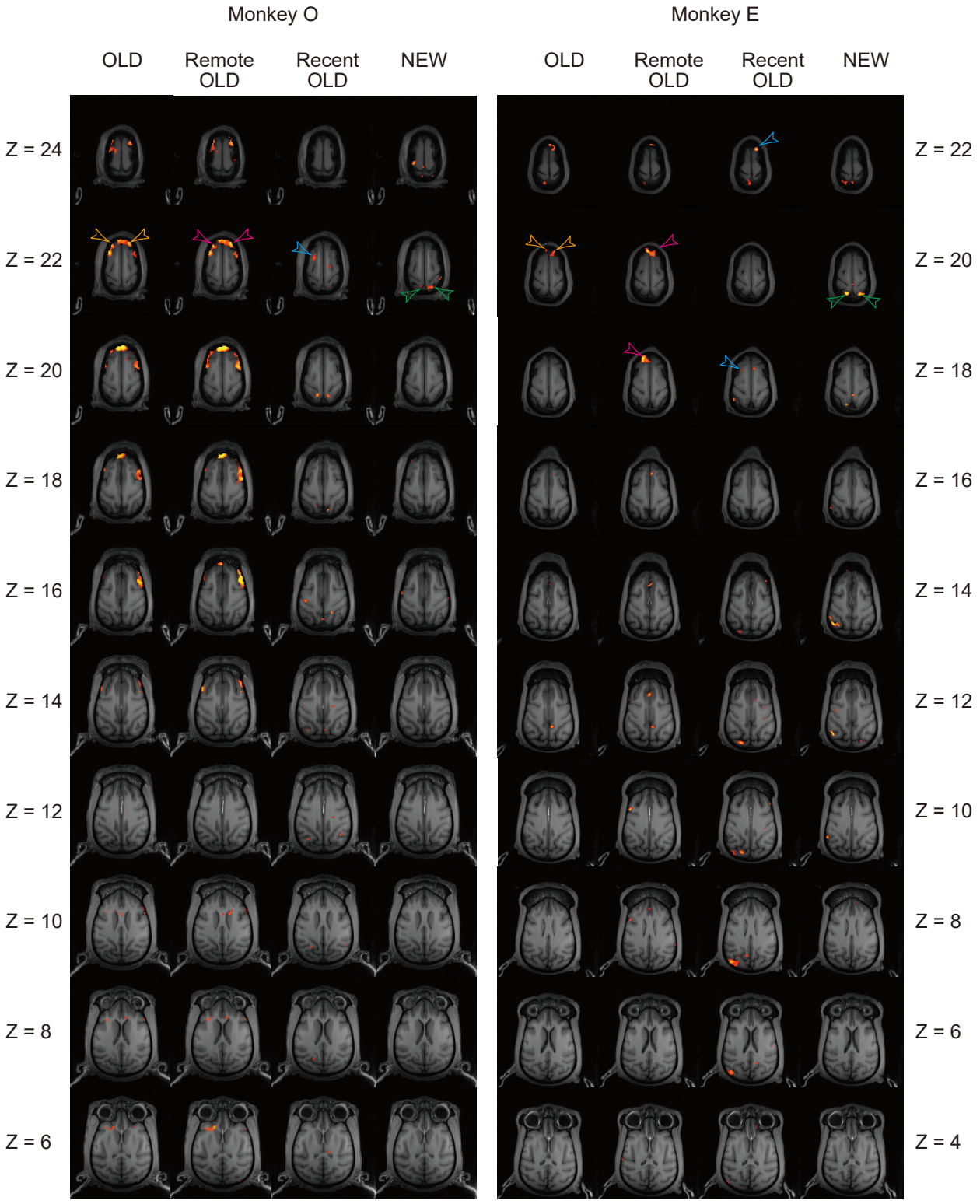

Figure S5 (1 of 2)

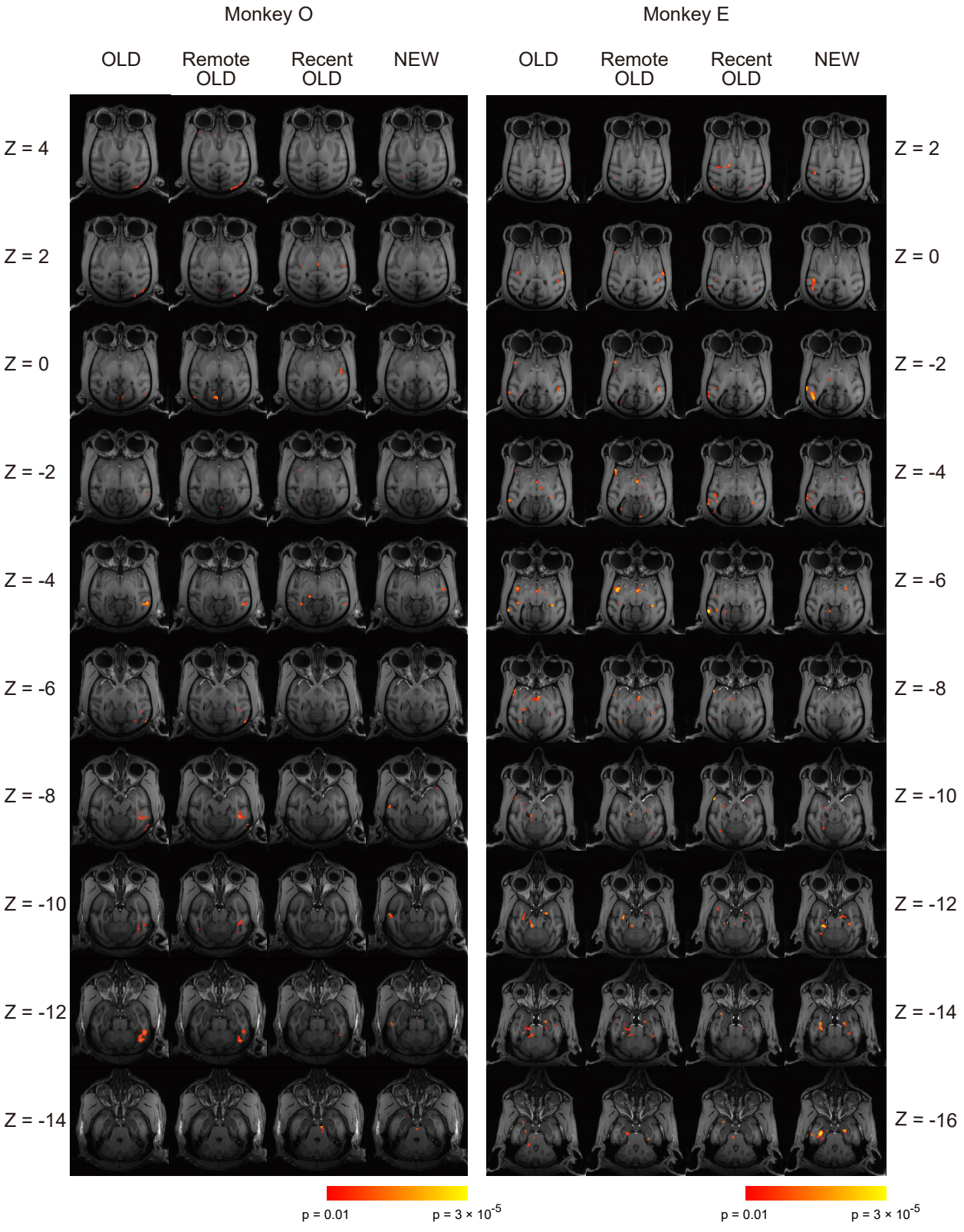

Figure S5 (2 of 2)

Fig. S5. Reproducibility of whole-brain activity patterns across subjects. Metamemory processing areas for OLD, Remote OLD, Recent OLD, and NEW conditions in individual animals thresholded for display purpose ($z > 2.3$, $p < 0.01$, uncorrected). The results are shown on the template 3D brain volume of respective monkeys (axial slices with 2 mm spacing that covered whole brain volume). Activation spots identified in the group analysis (listed in Table S1 and S2) were indicated by arrows (orange, area 9 / 9/46d in OLD condition; pink, aPSPD in Remote OLD condition; light blue, SEFa in Recent OLD condition; green, area 7 in NEW condition). See also Table S4 for the coordinates and statistical significance of activation peaks.

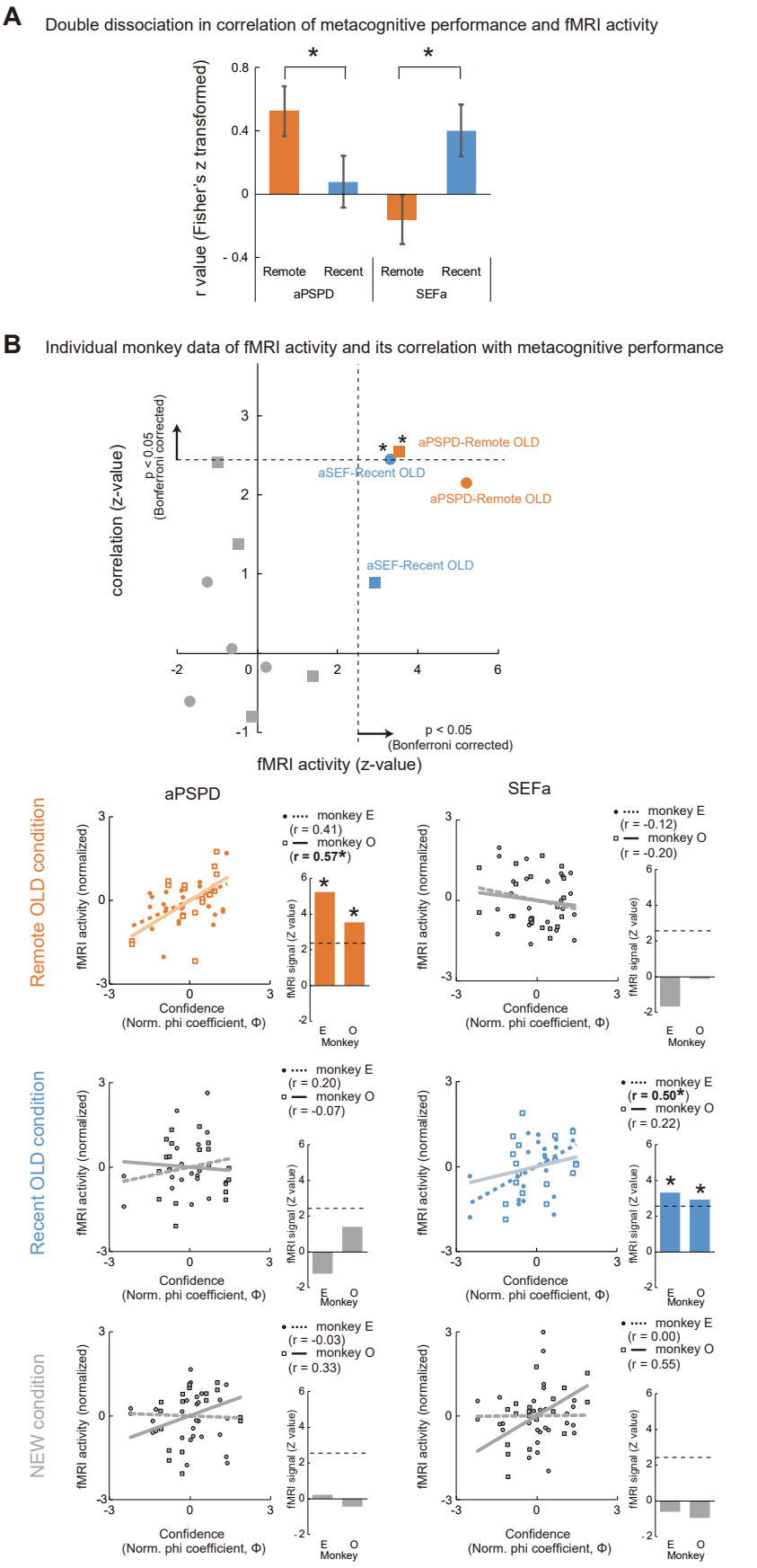
A
Double dissociation in correlation of metacognitive performance and fMRI activity
r value (Fisher's z transformed)
0.8
0.4
0
- 0.4
*
*
Remote
Recent
Remote
Recent
aPSPD
SEFa
B
Individual monkey data of fMRI activity and its correlation with metacognitive performance
correlation (z-value)
p < 0.05
(Bonferroni corrected)
aPSPD-Remote OLD
aSEF-Recent OLD
aPSPD-Remote OLD
aSEF-Recent OLD
p < 0.05
(Bonferroni corrected)
fMRI activity (z-value)
aPSPD
SEFa
Remote OLD condition
Recent OLD condition
NEW condition
fMRI activity (normalized)
Confidence
(Norm. phi coefficient, Φ)
monkey E
monkey O
(r = 0.41)
(r = 0.57*)
(r = -0.12)
(r = -0.20)
(r = 0.20)
(r = -0.07)
(r = 0.50*)
(r = 0.22)
(r = -0.03)
(r = 0.33)
(r = 0.00)
(r = 0.55)
fMRI signal (Z value)
E
O
Monkey

Figure S6

Fig. S6. Correlation between confidence judgment performance and brain activity. (**A**) Direct comparisons of the correlation coefficients between confidence judgment performance (phi-coefficient[Φ], z-transformed) and fMRI activity (high-bet vs. low-bet, z-transformed) by using Fisher's Z transformation. Interaction between areas (aPSPD and SEFa) and task condition (Remote and Recent OLD) was statistically significant ($p = 0.0015$). *, $p < 0.05$, paired-Z test. (**B**) Top, Relationship between fMRI activity (abscissa) and session-by-session correlation between fMRI activity and Φ (ordinate). Circle, monkey E; square, monkey O. Dotted lines depict statistical threshold of $p < 0.05$ with Bonferroni's correction. *, conditions showing statistically significant fMRI activity (aPSPD of Remote OLD in monkey O and aSEF of Recent OLD in monkey E) coupled with significant correlation. Bottom, inter-session correlation between confidence judgment performance (phi-coefficient[Φ], z-transformed) and fMRI activity (high-bet vs. low-bet, z-transformed). Correlation coefficients are shown separately for each animal. An analysis of covariance (ANCOVA) on fMRI activity (monkey × confidence) also confirmed that the correlation was consistent across animals for both aPSPD in Remote OLD condition and SEFa in Recent OLD condition: ANCOVA showed a significant main effect of confidence judgment performance (aPSPD in Remote OLD condition, $F_{1,40} = 12.17$, $p = 0.0012$; SEFa in Recent OLD condition, $F_{1,36} = 6.26$, $p = 0.017$) with no interaction between monkey and confidence (aPSPD in Remote OLD condition, $F_{1,40} = 0.34$, $p = 0.56$; SEFa in Recent OLD condition, $F_{1,36} = 0.86$, $p = 0.35$).

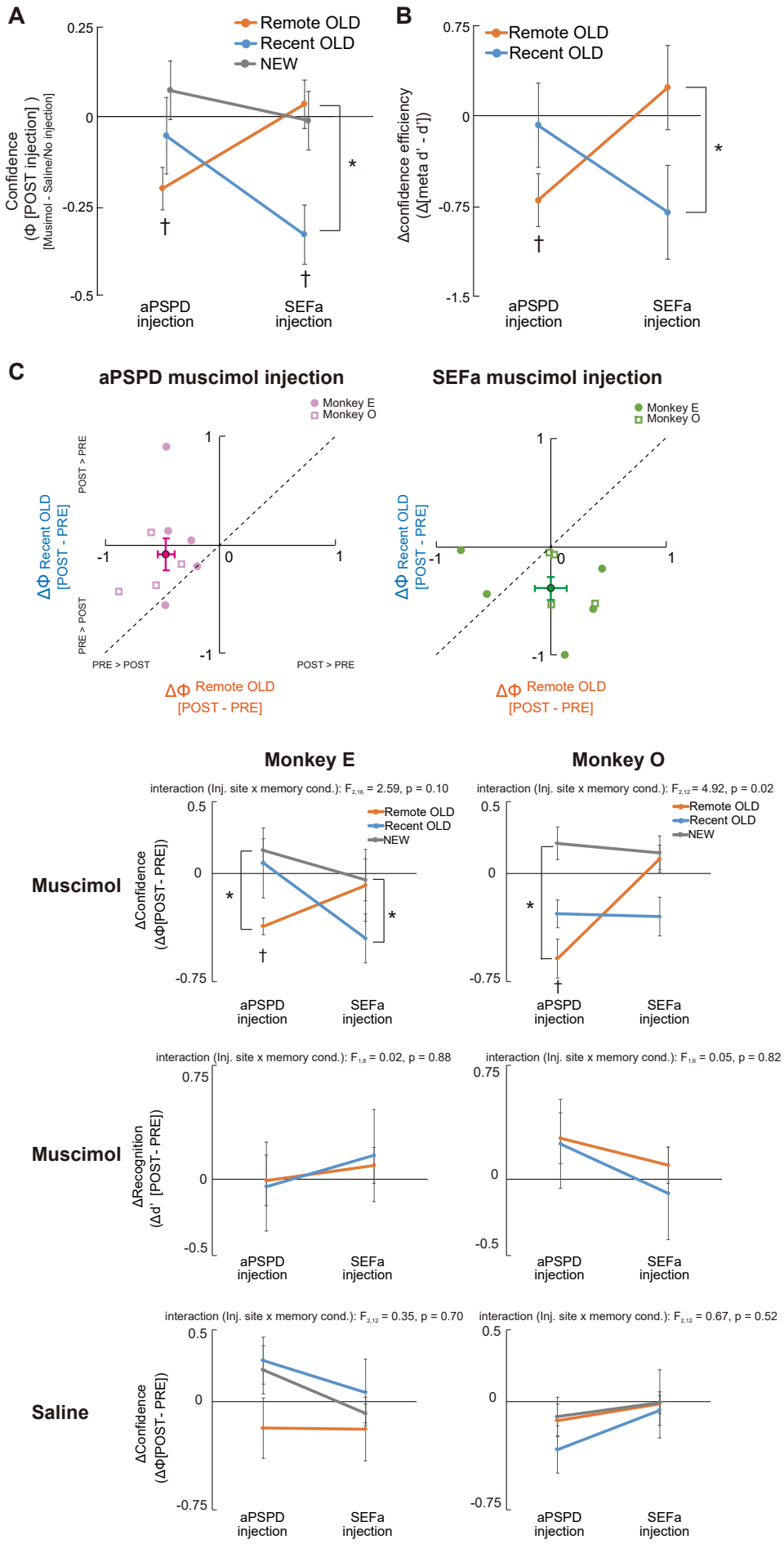
A
Remote OLD
Recent OLD
NEW
Confidence
(Φ [POST injection])
[Muscimol - Saline/No injection]
aPSPD injection
SEFa injection
B
Remote OLD
Recent OLD
Δconfidence efficiency
(Δ[meta d' - d'])
C
aPSPD muscimol injection
SEFa muscimol injection
Monkey E
Monkey O
ΔΦ Recent OLD [POST - PRE]
ΔΦ Remote OLD [POST - PRE]
POST > PRE
PRE > POST
Monkey E
Monkey O
interaction (Inj. site x memory cond.): F2,16 = 2.59, p = 0.10
interaction (Inj. site x memory cond.): F2,12 = 4.92, p = 0.02
Muscimol
ΔConfidence (ΔΦ[POST- PRE])
interaction (Inj. site x memory cond.): F1,8 = 0.02, p = 0.88
interaction (Inj. site x memory cond.): F1,6 = 0.05, p = 0.82
Muscimol
ΔRecognition (Δd' [POST- PRE])
interaction (Inj. site x memory cond.): F2,12 = 0.35, p = 0.70
interaction (Inj. site x memory cond.): F2,12 = 0.67, p = 0.52
Saline
ΔConfidence (ΔΦ[POST- PRE])

Figure S7

Fig. S7. Causal impact by reversible inactivation on metamnemonic performance. (**A**) Behavioral effects of muscimol injection evaluated using Φ after injection (Φ[POST injection], Muscimol – Saline/No Injection). The interaction for injected loci × memory task conditions was significant ($F_{2,28} = 3.90$, $p = 0.032$). *$p < 0.05$, paired *t*-test. †$p < 0.05$, *t*-test against zero. (**B**) Behavioral effects of muscimol injection evaluated by signal-detection theory-based metacognitive efficiency index Δ(meta-*d'* – *d'*) . The interaction for injected loci × memory task conditions was significant ($F_{1,7} = 6.41$, $p = 0.039$). *$p < 0.05$, paired *t*-test. †$p < 0.05$, *t*-test against zero. (**C**) Top, session-by-session evaluation of causal impact on confidence judgment performance for Remote and Recent OLD conditions after muscimol injection into the aPSPD (left) or SEFa (right). Each dot represents a single session in each monkey. A dot with error bars represents mean ± s.e.m. of causal impact across all sessions. Row second from top, performance change in confidence judgment following muscimol injection for each monkey. Interaction between injection site (aPSPD, SEFa) and memory condition (Remote OLD, Recent OLD, NEW) was significant in monkey O ($F_{2,12} = 4.92$, $p = 0.02$) and marginally significant but did not reach the threshold of $p < 0.05$ in monkey E ($F_{2,16} = 2.59$, $p = 0.10$). Configurations are the same as in Fig. 4B. Row third from top, performance changes in recognition memory following muscimol injection for each monkey. Configurations are the same as in Fig. 4D. Bottom, performance change in confidence judgment following saline injection for each monkey. Configurations are the same as in Fig. 4C. *$p < 0.05$, paired *t*-test, Ryan's correction. †$p < 0.05$, *t*-test against zero, Bonferroni's correction.

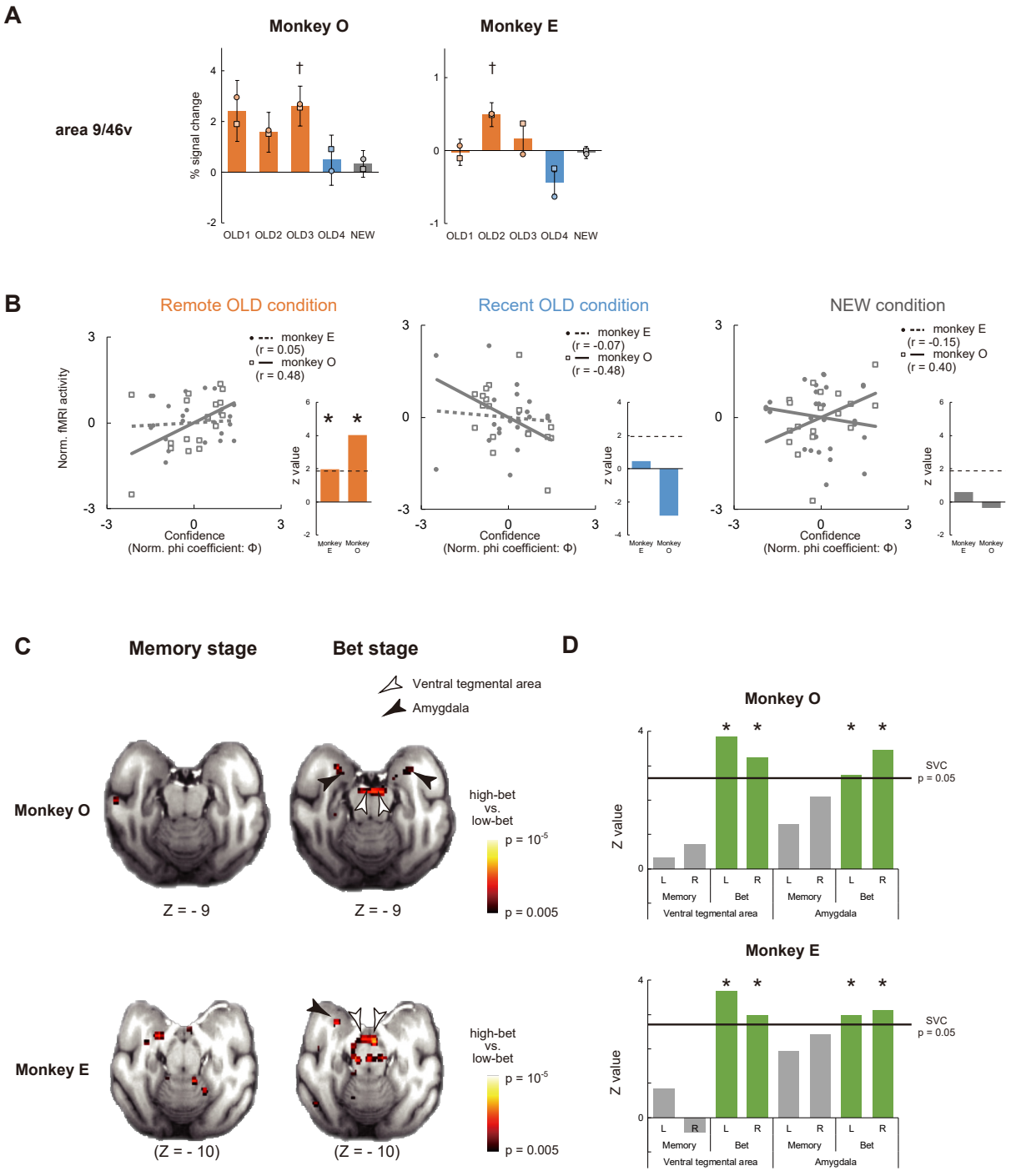
A
Monkey O
Monkey E
area 9/46v
% signal change
OLD1 OLD2 OLD3 OLD4 NEW
B
Remote OLD condition
Recent OLD condition
NEW condition
monkey E
(r = 0.05)
monkey O
(r = 0.48)
(r = -0.07)
(r = -0.48)
(r = -0.15)
(r = 0.40)
Norm. fMRI activity
Confidence
(Norm. phi coefficient: Φ)
z value
Monkey E
Monkey O
C
Memory stage
Bet stage
Ventral tegmental area
Amygdala
Monkey O
Monkey E
high-bet
vs.
low-bet
p = 10-5
p = 0.005
Z = - 9
(Z = - 10)
D
SVC
p = 0.05
Z value
L
R
Memory
Bet
Ventral tegmental area
Amygdala

Figure S8

Fig. S8. fMRI activity in an attention-related area and reward-related areas. (**A**–**B**) fMRI activity in an attention-related area (9/46v). (**A**) Percent signal changes (high-bet vs. low-bet trials) in each cue position of OLD conditions (OLD1–4) and in NEW conditions at bilateral 9/46v. Square, left area, circle, right area. † $p < 0.05$, *t*-test against zero, Bonferroni's correction. See also Supplementary text. (**B**) Inter-session correlation between confidence judgment performance (phi coefficient[Φ], z-transformed) and fMRI activity (high-bet vs. low-bet, z-transformed). Filled circle, monkey E; open square, monkey O. Statistical Z values of fMRI signals (high-bet vs. low-bet) were also shown at the right of the scatter plots. *$p < 0.05$ with Bonferroni's correction. See Supplemental text for details. (**C**–**D**) fMRI activity in reward-related areas (ventral tegmental area and amygdala) (**C**) Activation map of the reward-related areas (high-bet vs. low-bet for all correct trials) for Memory and Bet stages. $z > 2.57$, $p < 0.005$, uncorrected for display purpose. (**D**) Comparison of fMRI signals (high-bet vs. low-bet for all correct trials) of the ventral tegmental area and the amygdala in Memory stage (grey) and Bet stage (green). ROIs for these areas (2-mm radius) were defined based on Neubert et al. (*55*). *$p < 0.05$, FWE small volume corrected in each hemisphere of each monkey.

A Metamemory processing areas for OLD condition (high-bet vs. low-bet)

Left hemisphere				Right hemisphere				
x	y	z	Z value	x	y	z	Z value	area
-3	19	19	5.88*	6	15	17	2.64	9
-11	13	21	5.29*	13	11	22	3.59	9/9/46d
-17	7	19	3.67	17	6	16	5.09*	9/46v

B Metamemory processing areas for NEW condition (high-bet vs. low-bet)

Left hemisphere				Right hemisphere				
x	y	z	Z value	x	y	z	Z value	area
-11	-16	25	5.22*	10	-17	25	1.73	6 (PMdc)
-14	-28	21	5.19*	14	-29	20	2.77	7 (PG)

Table S1

Table S1. Metamemory processing areas for OLD and NEW conditions (high-bet vs. low-bet). Metamemory processing areas are separately shown for OLD condition (**A**) and NEW condition (**B**). Significant peaks were detected at the threshold of $p < 0.05$, corrected by family-wise error (FWE) across the whole brain volume. The homotopic peak in the contralateral hemisphere is also included in the table if it exists (see Methods). Coordinates are listed in monkey bicommissural space (*18, 19, 31-33*). *$p < 0.05$, FWE corrected across the whole brain.

A Metamemory processing areas for Remote OLD condition (high-bet vs. low-bet)

Left hemisphere				Right hemisphere				
x	y	z	Z value	x	y	z	Z value	area
-4	18	19	6.63*	5	18	20	4.66	9 (mPSPD)
-11	12	21	5.84*	8	11	23	4.83*	9/9/46d (aPSPD)
-17	7	19	3.68	18	6	16	5.62*	9/46v
-10	6	23	3.97	10	5	25	5.32*	8B/9
-17	1	20	4.46	15	0	21	5.14*	6 (PMv)

B Metamemory processing areas for Recent OLD condition (high-bet vs. low-bet)

Left hemisphere				Right hemisphere				
x	y	z	Z value	x	y	z	Z value	area
-9	2	21	5.11*	5	1	21	2.09	6 (SEFa)
-9	-22	14	2.98	8	-23	17	5.07*	5 (PEa/DIP)
-6	-27	19	5.14*	5	-27	21	5.13*	5 (PEa)

Table S2

Table S2. Metamemory processing areas for Remote and Recent OLD conditions (high-bet vs. low-bet). Metamemory processing areas are separately shown for Remote OLD condition (**A**) and Recent OLD condition (**B**). Significant peaks were detected at the threshold of $p < 0.05$, corrected by FWE across the whole brain volume. The homotopic peak in the contralateral hemisphere is also included in the table if it exists. *$p < 0.05$, FWE corrected across the whole brain.

Ipsilateral connectivity

seed	target areas	seed L / R	x	y	z	Z value
aPSPD (Remote OLD)	**Inferior parietal lobule (PG)**	L	-14	-29	21	4.15*
		R	14	-29	20	2.36†
	Frontopolar prefrontal cortex (10)	L	-6	26	8	4.05*
	Extrastriate cortex (V2)	L	-12	-28	0	3.82*
SEFa (Recent OLD)	**Superior parietal lobule (PEa)**	L	-8	-30	20	3.57†
		R	8	-32	20	3.82*

Contralateral connectivity

seed	target areas	seed L / R	x	y	z	Z value
aPSPD (Remote OLD)	Inferior parietal lobule (PG)	R	-15	-28	20	4.57*
	Inferior temporal cortex (TEav)	R	-21	-10	-16	4.20*
	Extrastriate cortex (V2)	R	-22	-33	-1	3.46*
SEFa (Recent OLD)	Superior parietal lobule (PEa)	L	8	-31	20	6.07*

Table S3

Table S3. Task-evoked connectivity for Remote and Recent OLD conditions (high-bet vs. low-bet). Task-evoked connectivity (psychophysiological interaction [PPI]) in response to metamemory processes in memory retrieval. The PPIs with a seed at the aPSPD and SEFa were calculated in Remote OLD condition and Recent OLD condition, respectively. Significant peaks of PPI at the cluster-level of $p < 0.05$, corrected by false discovery rate (FDR) across the whole brain, are listed in the table. *$p < 0.05$, FDR corrected at the cluster-level across the whole brain. †$p < 0.05$, FWE corrected for small volume (detected in the contralateral region for each significant PPI peak).

A Metamemory processing areas for OLD condition (high-bet vs. low-bet)

Monkey O

Left hemisphere				Right hemisphere				
x	y	z	Z value	x	y	z	Z value	area
-4	18	20	4.48*	1	19	20	4.15*(§1)	9
-10	15	22	4.21*	8	15	22	4.07*(§2)	9/9/46d
-12	6	22	3.59	17	6	17	3.96*	9/46v

Monkey E

Left hemisphere				Right hemisphere				
x	y	z	Z value	x	y	z	Z value	area
-2	7	20	2.72	4	7	20	2.29	9
-6	11	19	2.66	5	6	21	3.26	9/9/46d
	(#1)				(#2)			9/46v

B Metamemory processing areas for NEW condition (high-bet vs. low-bet)

Monkey O

Left hemisphere				Right hemisphere				
x	y	z	Z value	x	y	z	Z value	area
-11	-16	25	3.88*	14	-20	22	2.43	6 (PMdc)
-16	-23	23	2.98	10	-27	23	2.74	7 (PG)

Monkey E

Left hemisphere				Right hemisphere				
x	y	z	Z value	x	y	z	Z value	area
-8	-25	23	2.17			(#3)		6 (PMdc)
-15	-31	21	2.77	13	-35	21	3.75*	7 (PG)

C Metamemory processing areas for Remote OLD condition (high-bet vs. low-bet)

Monkey O

Left hemisphere				Right hemisphere				
x	y	z	Z value	x	y	z	Z value	area
-3	19	20	4.86*	2	19	20	4.54*	9 (mPSPD)
-12	13	22	4.15*	8	15	22	4.39*	9/9/46d (aPSPD)
-19	9	15	3.39	17	7	17	4.27*	9/46v
-12	11	22	3.89*	10	5	24	3.73*	8B/9
-13	4	22	3.67*	18	-1	18	3.88*	6 (PMv)

Monkey E

Left hemisphere				Right hemisphere				
x	y	z	Z value	x	y	z	Z value	area
-2	7	20	3.98*	5	7	21	2.83	9 (mPSPD)
-7	9	18	3.97*	3	3	22	3.71*	9/9/46d (aPSPD)
-16	3	11	1.73			(#4)		9/46v
-7	5	18	3.01	5	2	21	2.72	8B/9
	(#5)			11	1	21	2.14	6 (PMv)

D Metamemory processing areas for Recent OLD condition (high-bet vs. low-bet)

Monkey O

Left hemisphere				Right hemisphere				
x	y	z	Z value	x	y	z	Z value	area
-9	3	21	3.14	3	-4	23	2.07	6 (SEFa)
-11	-25	16	2.60	8	-23	16	3.41	5 (PEa/DIP)
-6	-27	19	3.67*	5	-27	21	3.56	5 (PEa)

Monkey E

Left hemisphere				Right hemisphere				
x	y	z	Z value	x	y	z	Z value	area
-8	-3	18	2.56	5	-2	24	4.85*	6 (SEFa)
-7	-28	13	1.76	4	-26	12	2.22	5 (PEa/DIP)
-3	-31	23	2.89	0	-34	22	2.42	5 (PEa)

E Task-evoked connectivity for Remote and Recent OLD conditions (high-bet vs. low-bet)

Monkey O

Ipsilateral connectivity

seed	target areas	seed L / R	x	y	z	Z value
aPSPD (Remote OLD)	**Inferior parietal lobule (PG)**	L	-14	-29	21	3.15
		R	14	-33	18	2.36
	Frontopolar prefrontal cortex (10)	L	-3	24	3	4.16*
	Extrastriate cortex (V2)	L	-13	-27	2	2.98
SEFa (Recent OLD)	**Superior parietal lobule (PEa)**	L	-3	-32	20	3.66*
		R	5	-33	21	3.86*

Contralateral connectivity

seed	target areas	seed L / R	x	y	z	Z value
aPSPD (Remote OLD)	Inferior parietal lobule (PG)	R	-15	-28	20	3.48
	Inferior temporal cortex (TEav)	R	-22	-11	-16	4.09*
	Extrastriate cortex (V2)	R	-18	-36	-3	3.11
SEFa (Recent OLD)	Superior parietal lobule (PEa)	L	8	-30	20	5.40*

Monkey E

Ipsilateral connectivity

seed	target areas	seed L / R	x	y	z	Z value
aPSPD (Remote OLD)	**Inferior parietal lobule (PG)**	L	-9	-33	23	4.71*
		R	15	-34	19	3.25
	Frontopolar prefrontal cortex (10)	L	-7	14	5	3.38
	Extrastriate cortex (V2)	L	-12	-33	0	4.92*
SEFa (Recent OLD)	**Superior parietal lobule (PEa)**	L	-6	-35	19	4.31*
		R	11	-33	23	5.33*

Contralateral connectivity

seed	target areas	seed L / R	x	y	z	Z value
aPSPD (Remote OLD)	Inferior parietal lobule (PG)	R	-10	-32	22	3.73*
	Inferior temporal cortex (TEav)	R	-16	-20	-17	2.42
	Extrastriate cortex (V2)	R	-24	-34	-3	4.46*
SEFa (Recent OLD)	Superior parietal lobule (PEa)	L	11	-33	23	5.62*

#1, x = -19, y = -1, z = 10, Z value = 2.21; #2, x = 12, y = 1, z = 21, Z value = 2.75; #3, x = 3, y = -25, z = 20, Z value = 1.91; #4, x = 7, y = 11, z = 13, Z value = 1.92; #5, x = -6, y = -2, z = 22, Z value = 1.90.

Table S4

Table S4. Metamemory processing areas and task-evoked connectivity in individual animals. Metamemory processing areas for OLD (**A**), NEW (**B**), Remote OLD (**C**), and Recent OLD (**D**) conditions (see Table S1 and S2), and task-evoked connectivity (**E**) (see Table S3) are shown in individual animals. Significant peaks ($p < 0.05$) of individual animals, which were detected within 6 mm-radius sphere around the peaks of group analyses, are listed. The coordinates are shown in the respective monkey's bicommissural space (see also Fig. S5). *$p < 0.05$, FWE corrected for small volume. §1 and §2: As nearly identical peaks were detected for these two areas, significant peaks were re-detected within 6 mm-radius sphere around the x-flipped contralateral peaks that survived FWE whole-brain correction. #1 - #5: significant peak was not detected within 6 mm-radius sphere; the nearest significant peak is shown at the bottom of the table.

References and Notes

1. L. R. Squire, B. Knowlton, G. Musen, The structure and organization of memory. *Annu. Rev. Psychol.* **44**, 453–495 (1993). doi:10.1146/annurev.ps.44.020193.002321 Medline

2. S. Dehaene, *The Cognitive Neuroscience of Consciousness* (MIT Press, Cambridge, MA, 2001).

3. M. Petrides, Lateral prefrontal cortex: Architectonic and functional organization. *Philos. Trans. R. Soc. Lond. B Biol. Sci.* **360**, 781–795 (2005). doi:10.1098/rstb.2005.1631 Medline

4. J. I. Gold, M. N. Shadlen, The neural basis of decision making. *Annu. Rev. Neurosci.* **30**, 535–574 (2007). doi:10.1146/annurev.neuro.29.051605.113038 Medline

5. M. F. Rushworth, N. Kolling, J. Sallet, R. B. Mars, Valuation and decision-making in frontal cortex: One or many serial or parallel systems? *Curr. Opin. Neurobiol.* **22**, 946–955 (2012). doi:10.1016/j.conb.2012.04.011 Medline

6. Y. Miyashita, Cognitive memory: Cellular and network machineries and their top-down control. *Science* **306**, 435–440 (2004). doi:10.1126/science.1101864 Medline

7. T. O. Nelson, Metamemory: A theoretical framework and new findings. *Psychol. Learn. Motiv.* **26**, 125–173 (1990). doi:10.1016/S0079-7421(08)60053-5

8. A. P. Shimamura, L. R. Squire, Memory and metamemory: A study of the feeling-of-knowing phenomenon in amnesic patients. *J. Exp. Psychol. Learn. Mem. Cogn.* **12**, 452–460 (1986). doi:10.1037/0278-7393.12.3.452 Medline

9. R. Passingham, How good is the macaque monkey model of the human brain? *Curr. Opin. Neurobiol.* **19**, 6–11 (2009). doi:10.1016/j.conb.2009.01.002 Medline

10. H. Tomita, M. Ohbayashi, K. Nakahara, I. Hasegawa, Y. Miyashita, Top-down signal from prefrontal cortex in executive control of memory retrieval. *Nature* **401**, 699–703 (1999). doi:10.1038/44372 Medline

11. W. Vanduffel, Q. Zhu, G. A. Orban, Monkey cortex through fMRI glasses. *Neuron* **83**, 533–550 (2014). doi:10.1016/j.neuron.2014.07.015 Medline

12. R. R. Hampton, Multiple demonstrations of metacognition in nonhumans: Converging evidence or multiple mechanisms? *Comp. Cogn. Behav. Rev.* **4**, 17–28 (2009). doi:10.3819/ccbr.2009.40002 Medline

13. J. D. Smith, W. E. Shields, K. R. Allendoerfer, D. A. Washburn, Memory monitoring by animals and humans. *J. Exp. Psychol. Gen.* **127**, 227–250 (1998). doi:10.1037/0096-3445.127.3.227 Medline

14. A. Kepecs, N. Uchida, H. A. Zariwala, Z. F. Mainen, Neural correlates, computation and behavioural impact of decision confidence. *Nature* **455**, 227–231 (2008). doi:10.1038/nature07200 Medline

15. R. Kiani, M. N. Shadlen, Representation of confidence associated with a decision by neurons in the parietal cortex. *Science* **324**, 759–764 (2009). doi:10.1126/science.1169405 Medline

16. C. R. Fetsch, R. Kiani, W. T. Newsome, M. N. Shadlen, Effects of cortical microstimulation on confidence in a perceptual decision. *Neuron* **83**, 797–804 (2014). doi:10.1016/j.neuron.2014.07.011 Medline

17. P. G. Middlebrooks, M. A. Sommer, Neuronal correlates of metacognition in primate frontal cortex. *Neuron* **75**, 517–530 (2012). doi:10.1016/j.neuron.2012.05.028 Medline

18. K. Miyamoto, T. Osada, Y. Adachi, T. Matsui, H. M. Kimura, Y. Miyashita, Functional differentiation of memory retrieval network in macaque posterior parietal cortex. *Neuron* **77**, 787–799 (2013). doi:10.1016/j.neuron.2012.12.019 Medline

19. K. Miyamoto, Y. Adachi, T. Osada, T. Watanabe, H. M. Kimura, R. Setsuie, Y. Miyashita, Dissociable memory traces within the macaque medial temporal lobe predict subsequent recognition performance. *J. Neurosci.* **34**, 1988–1997 (2014). doi:10.1523/JNEUROSCI.4048-13.2014 Medline

20. R. R. Hampton, A. Zivin, E. A. Murray, Rhesus monkeys (*Macaca mulatta*) discriminate between knowing and not knowing and collect information as needed before acting. *Anim. Cogn.* **7**, 239–246 (2004). doi:10.1007/s10071-004-0215-1 Medline

21. P. G. Middlebrooks, M. A. Sommer, Metacognition in monkeys during an oculomotor task. *J. Exp. Psychol. Learn. Mem. Cogn.* **37**, 325–337 (2011). doi:10.1037/a0021611 Medline

22. B. Maniscalco, H. Lau, A signal detection theoretic approach for estimating metacognitive sensitivity from confidence ratings. *Conscious. Cogn.* **21**, 422–430 (2012). doi:10.1016/j.concog.2011.09.021 Medline

23. N. Caspari, T. Janssens, D. Mantini, R. Vandenberghe, W. Vanduffel, Covert shifts of spatial attention in the macaque monkey. *J. Neurosci.* **35**, 7695–7714 (2015). doi:10.1523/JNEUROSCI.4383-14.2015 Medline

24. D. Kaping, M. Vinck, R. M. Hutchison, S. Everling, T. Womelsdorf, Specific contributions of ventromedial, anterior cingulate, and lateral prefrontal cortex for attentional selection and stimulus valuation. *PLOS Biol.* **9**, e1001224 (2011). doi:10.1371/journal.pbio.1001224 Medline

25. M. Petrides, Monitoring of selections of visual stimuli and the primate frontal cortex. *Proc. Biol. Sci.* **246**, 293–298 (1991). doi:10.1098/rspb.1991.0157 Medline

26. M. Petrides, Functional specialization within the dorsolateral frontal cortex for serial order memory. *Proc. Biol. Sci.* **246**, 299–306 (1991). doi:10.1098/rspb.1991.0158 Medline

27. J. Sallet, R. B. Mars, M. P. Noonan, F.-X. Neubert, S. Jbabdi, J. X. O'Reilly, N. Filippini, A. G. Thomas, M. F. Rushworth, The organization of dorsal frontal cortex in humans and macaques. *J. Neurosci.* **33**, 12255–12274 (2013). doi:10.1523/JNEUROSCI.5108-12.2013 Medline

28. S. M. Fleming, R. S. Weil, Z. Nagy, R. J. Dolan, G. Rees, Relating introspective accuracy to individual differences in brain structure. *Science* **329**, 1541–1543 (2010). doi:10.1126/science.1191883 Medline

29. S. M. Fleming, J. Ryu, J. G. Golfinos, K. E. Blackmon, Domain-specific impairment in metacognitive accuracy following anterior prefrontal lesions. *Brain* **137**, 2811–2822 (2014). doi:10.1093/brain/awu221 Medline

30. F.-X. Neubert, R. B. Mars, A. G. Thomas, J. Sallet, M. F. Rushworth, Comparison of human ventral frontal cortex areas for cognitive control and language with areas in monkey frontal cortex. *Neuron* **81**, 700–713 (2014). doi:10.1016/j.neuron.2013.11.012 Medline

31. K. Nakahara, T. Hayashi, S. Konishi, Y. Miyashita, Functional MRI of macaque monkeys performing a cognitive set-shifting task. *Science* **295**, 1532–1536 (2002). doi:10.1126/science.1067653 Medline

32. M. Koyama, I. Hasegawa, T. Osada, Y. Adachi, K. Nakahara, Y. Miyashita, Functional magnetic resonance imaging of macaque monkeys performing visually guided saccade tasks: Comparison of cortical eye fields with humans. *Neuron* **41**, 795–807 (2004). doi:10.1016/S0896-6273(04)00047-9 Medline

33. T. Osada, Y. Adachi, K. Miyamoto, K. Jimura, R. Setsuie, Y. Miyashita, Dynamically allocated hub in task-evoked network predicts the vulnerable prefrontal locus for contextual memory retrieval in macaques. *PLOS Biol.* **13**, e1002177 (2015). doi:10.1371/journal.pbio.1002177 Medline

34. T. Hirabayashi, D. Takeuchi, K. Tamura, Y. Miyashita, Microcircuits for hierarchical elaboration of object coding across primate temporal areas. *Science* **341**, 191–195 (2013). doi:10.1126/science.1236927 Medline

35. M. Takeda, K. W. Koyano, T. Hirabayashi, Y. Adachi, Y. Miyashita, Top-down regulation of laminar circuit via inter-area signal for successful object memory recall in monkey temporal cortex. *Neuron* **86**, 840–852 (2015). doi:10.1016/j.neuron.2015.03.047 Medline

36. A. A. Wright, H. C. Santiago, S. F. Sands, D. F. Kendrick, R. G. Cook, Memory processing of serial lists by pigeons, monkeys, and people. *Science* **229**, 287–289 (1985). doi:10.1126/science.9304205 Medline

37. N. Kornell, L. K. Son, H. S. Terrace, Transfer of metacognitive skills and hint seeking in monkeys. *Psychol. Sci.* **18**, 64–71 (2007). doi:10.1111/j.1467-9280.2007.01850.x Medline

38. W. E. Shields, J. D. Smith, K. Guttmannova, D. A. Washburn, Confidence judgments by humans and rhesus monkeys. *J. Gen. Psychol.* **132**, 165–186 (2005). Medline

39. A. D. Wagner, J. E. Desmond, G. H. Glover, J. D. Gabrieli, Prefrontal cortex and recognition memory. Functional-MRI evidence for context-dependent retrieval processes. *Brain* **121**, 1985–2002 (1998). doi:10.1093/brain/121.10.1985 Medline

40. N. A. Macmillan, C. D. Creelman, *Detection Theory: A User's Guide* (Psychology Press, Hove, UK, 2004).

41. B. Baird, J. Smallwood, K. J. Gorgolewski, D. S. Margulies, Medial and lateral networks in anterior prefrontal cortex support metacognitive ability for memory and perception. *J. Neurosci.* **33**, 16657–16665 (2013). doi:10.1523/JNEUROSCI.0786-13.2013 Medline

42. E. D. Burgund, H. M. Lugar, F. M. Miezin, S. E. Petersen, Sustained and transient activity during an object-naming task: A mixed blocked and event-related fMRI study. *Neuroimage* **19**, 29–41 (2003). doi:10.1016/S1053-8119(03)00061-2 Medline

43. G. Paxinos, X.-F. Huang, M. Petrides, A. W. Toga, *The Rhesus Monkey Brain in Stereotaxic Coordinates* (Elsevier Academic, London, 2008).

44. T. Nichols, M. Brett, J. Andersson, T. Wager, J.-B. Poline, Valid conjunction inference with the minimum statistic. *Neuroimage* **25**, 653–660 (2005). doi:10.1016/j.neuroimage.2004.12.005 Medline

45. K. J. Friston, C. Buechel, G. R. Fink, J. Morris, E. Rolls, R. J. Dolan, Psychophysiological and modulatory interactions in neuroimaging. *Neuroimage* **6**, 218–229 (1997). doi:10.1006/nimg.1997.0291 Medline

46. J. R. Chumbley, K. J. Friston, False discovery rate revisited: FDR and topological inference using Gaussian random fields. *Neuroimage* **44**, 62–70 (2009). doi:10.1016/j.neuroimage.2008.05.021 Medline

47. K. J. Worsley, A. C. Evans, S. Marrett, P. Neelin, A three-dimensional statistical analysis for CBF activation studies in human brain. *J. Cereb. Blood Flow Metab.* **12**, 900–918 (1992). doi:10.1038/jcbfm.1992.127 Medline

48. B. K. Chau, J. Sallet, G. K. Papageorgiou, M. P. Noonan, A. H. Bell, M. E. Walton, M. F. Rushworth, Contrasting roles for orbitofrontal cortex and amygdala in credit assignment and learning in macaques. *Neuron* **87**, 1106–1118 (2015). doi:10.1016/j.neuron.2015.08.018 Medline

49. I. C. Van Dromme, E. Premereur, B.-E. Verhoef, W. Vanduffel, P. Janssen, Posterior parietal cortex drives inferotemporal activations during three-dimensional object vision. *PLOS Biol.* **14**, e1002445 (2016). doi:10.1371/journal.pbio.1002445 Medline

50. S. Moeller, W. A. Freiwald, D. Y. Tsao, Patches with links: A unified system for processing faces in the macaque temporal lobe. *Science* **320**, 1355–1359 (2008). doi:10.1126/science.1157436 Medline

51. R. Passingham, *What Is Special About the Human Brain?* (Oxford Univ. Press, Oxford, 2008).

52. N. K. Logothetis, What we can do and what we cannot do with fMRI. *Nature* **453**, 869–878 (2008). doi:10.1038/nature06976 Medline

53. J. Schlag, M. Schlag-Rey, Evidence for a supplementary eye field. *J. Neurophysiol.* **57**, 179–200 (1987). Medline

54. L. L. Chen, S. P. Wise, Neuronal activity in the supplementary eye field during acquisition of conditional oculomotor associations. *J. Neurophysiol.* **73**, 1101–1121 (1995). Medline

55. F.-X. Neubert, R. B. Mars, J. Sallet, M. F. Rushworth, Connectivity reveals relationship of brain areas for reward-guided learning and decision making in human and monkey frontal cortex. *Proc. Natl. Acad. Sci. U.S.A.* **112**, E2695–E2704 (2015). doi:10.1073/pnas.1410767112 Medline